少数粒子反応と最近の話題
Reaction in Few-Body System and Recent Topics

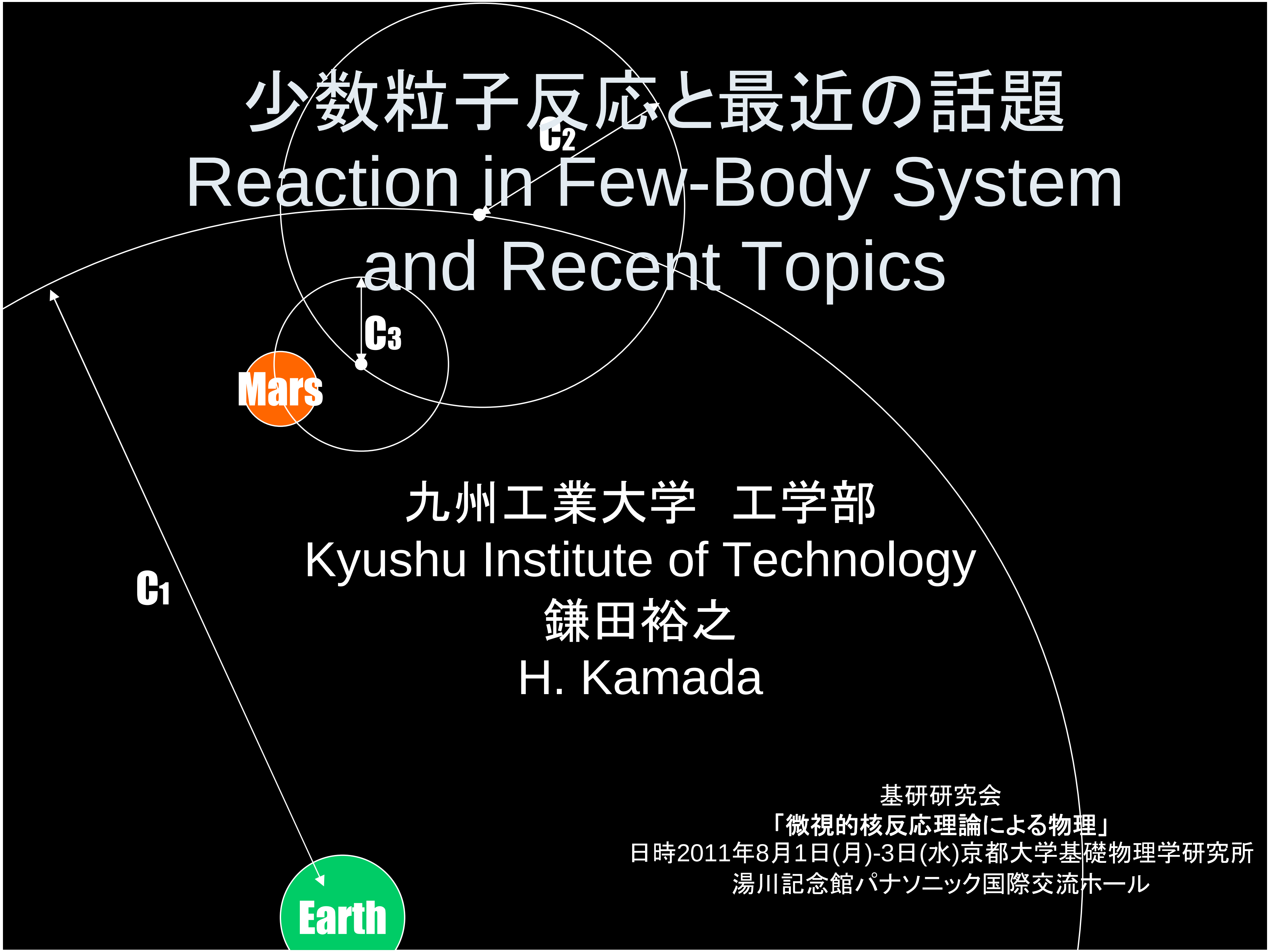

九州工業大学　工学部
Kyushu Institute of Technology
鎌田裕之
H. Kamada

基研研究会
「微視的核反応理論による物理」
日時2011年8月1日(月)-3日(水)京都大学基礎物理学研究所
湯川記念館パナソニック国際交流ホール

内容 content

- ３体力 :Three-body force

  ３体力を含むFaddeev方程式 :Faddeev equation

  カイラル有効場3体力: Chiral effective field theoritical 3-body force

  （１）NNLO

  （2）NNNLO　　(News 1)
- 相対論的3体計算: Reltivity in 3-body system

  （１）質量演算子: mass operator

  （2）3体力を含めた計算　(News 2)

３体力の重要性
Importance of ３－Body Force

- ２体力のみでの計算では、３核子系の束縛状態（３He、３H）の結合エネルギーの欠如。

  Under bound of 3He and 3H only by 2NF.

- どんな2体力や3体力を入力しても3N散乱状態を解くプログラムが出来上がった。

Develop of computer codes for 3-body scattering including with 3NF.

3体力を含む非相対論的3体方程式 Nonrelativistic Faddeev 3body eq. with 3NF

- Phys.Rep. 274, 107 (1996),
- Acta Phys. Pol. B28, 1677 (1997)

$$V = \sum_{i=1}^{3} V_i$$

２体力

$$V_4 = \sum_{i=1}^{3} V_4^{(i)}$$

３体力

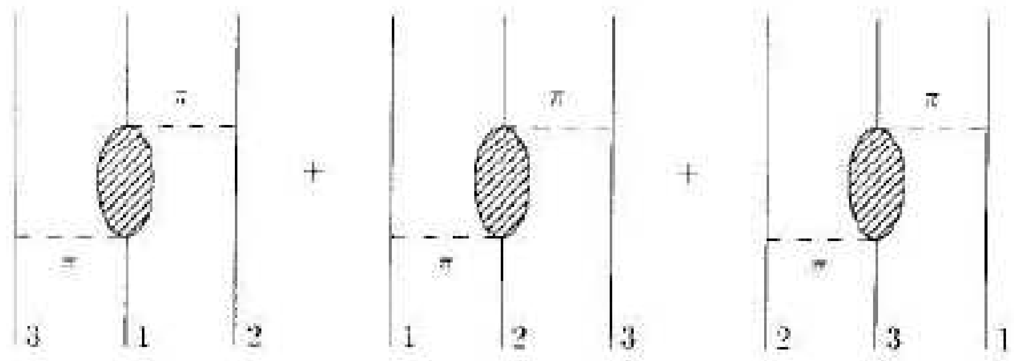

NdチャンネルがU始状態の散乱解Ψ Solution of scattering from the Nd initial channel

$$\Psi = G_0 \sum_{i=1}^{3} (V_i + V_4^{(i)})\Psi \equiv \sum_{i=1}^{3} \psi_i$$

$$\psi_i \equiv G_0 (V_i + V_4^{(i)})\Psi$$ - Faddeev component

$G_0 = 1/(E - H_0)$ は3体の自由グリーン関数

２体問題では意識しないが、3体問題以上ではSchroedinger方程式を満たすというだけの解は、ユニークにならない。境界条件が必要。

Faddeev component ψ_1

$$\psi_1 = G_0(V_1 + V_4^{(1)})(\psi_1 + \psi_2 + \psi_3)$$

２体の散乱行列tを用いると、

NN t-matrix t_1 related to V_1: $\quad t_1 = V_1 + V_1 G_0 t_1$

$$\psi_1 = \phi_1 + G_0 t_1(\psi_2 + \psi_3) + (1 + G_0 t_1) G_0 V_4^{(1)}(\psi_1 + \psi_2 + \psi_3)$$

を得る。

ϕ_1 は、Ndの始状態を意味する。:Nd initial state.

同一粒子:identical particle

$$P=P_{12}P_{23}+P_{13}P_{23}$$ 置換演算子:permutation operator

$$\psi_2+\psi_3=P\psi_1$$

粒子チャンネルのラベルを取る。: drop the particle label.

$$\psi_1=\phi_1+G_0t_1(\psi_2+\psi_3)+(1+G_0t_1)G_0V_4^{(1)}(\psi_1+\psi_2+\psi_3)$$

$$=\phi+G_0T$$

$$T\equiv tP\psi+(1+tG_0)V_4^{(1)}(1+P)\psi$$

代入する。
Tについての
方程式にする。

substitution

Faddeev eq. with 3NF

$$\boxed{\begin{aligned} T &= tP\phi + (1+tG_0)V_4^{(1)}(1+P)\phi \\ &+ tPG_0T + (1+tG_0)V_4^{(1)}(1+P)G_0T \end{aligned}}$$

$U_0 = (1+P)T$ 3体分解反応の散乱振幅 Break up amplitute

$$U = PG_0^{-1}\phi + PT + V_4^{(1)}(1+P)\phi + V_4^{(1)}(1+P)G_0T$$

弾性散乱の散乱振幅:scattering amplitude for elastic process

部分波表現:Partial wave decomp.

$$\left|pq\alpha\right\rangle \equiv \left|pqa\right\rangle \left|(t\frac{1}{2})T\right\rangle = \left|pq(ls)j(\lambda\frac{1}{2})I(jI)J(t\frac{1}{2})T\right\rangle$$

$$\sum_{\alpha}\int_{0}^{\infty}dpp^{2}\int_{0}^{\infty}dqq^{2}\left|pq\alpha\right\rangle\left\langle pq\alpha\right| = \mathrm{I}$$

完備性：Completeness

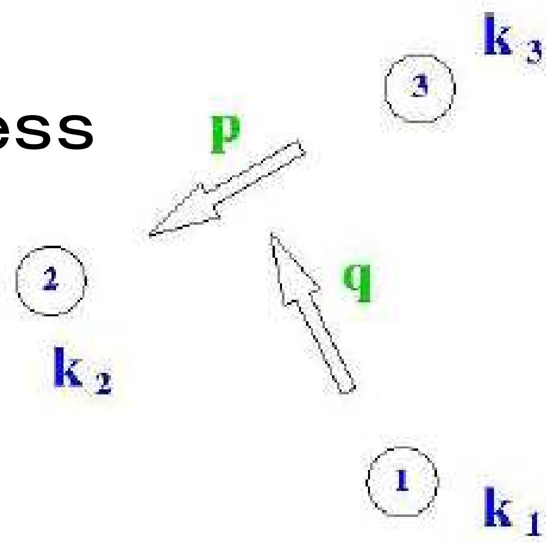

p.q; Jacobian coordinates

p、qは、それぞれ2体3体のヤコビ座標

The resulting set of coupled integral equations:

$$\langle pq\alpha|\hat{T}|\phi\rangle = \langle pq\alpha|\hat{t}P|\phi\rangle + \sum_{\alpha'}\sum_{\alpha''}\int_0^{\infty} dq' q'^2 \int_{-1}^{+1} dx \frac{\hat{t}_{\alpha_2\alpha_2'}(p,\pi_1,E-\frac{3}{4m}q^2)}{\pi_1^{l'}}$$

$$\times G_{\alpha'\alpha''}(qq'x)\frac{1}{E+i\varepsilon-\frac{q^2}{m}-\frac{q'^2}{m}-\frac{qq'x}{m}}$$

$$\times(\delta_{\alpha''\alpha_d}\frac{\langle\pi_2 q'\alpha''|\hat{T}|\phi\rangle}{\pi_2^{l''}}\frac{1}{E+i\varepsilon-\frac{3}{4m}q^2-\varepsilon_d}+\bar{\delta}_{\alpha''\alpha_d}\frac{\langle\pi_2 q'\alpha''|\hat{T}|\phi\rangle}{\pi_2^{l''}})$$

- coupled set of integral equations in 2 continuous variables for amplitudes $\langle pq\alpha|T|\phi\rangle$
- finite range of nuclear interaction $\longrightarrow$ finite number of channels α
- with $j_{max}=5$ about 150 coupled integral equations
- solved be generating Neuman series which is then summed up by Pade method

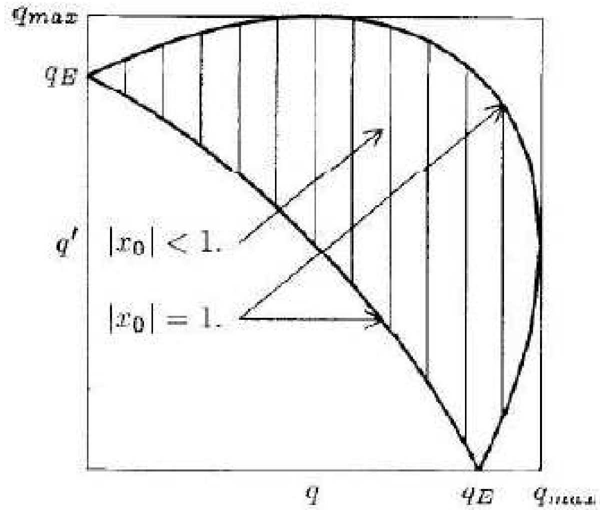

特異点（１） ：Singularities

W. Glöckle et al. / Physics Reports 274 (1996) 107–285 145

$$\frac{1}{E + i\epsilon - p''^{\,2}/m - (3/4m)q''^{\,2}} \, \frac{1}{E + i\epsilon - (3/4m)q''^{\,2} - \epsilon_d}$$

$$= \left\{ \frac{1}{E + i\epsilon - p''^{\,2}/m - (3/4m)q''^{\,2}} - \frac{1}{E + i\epsilon - (3/4m)q''^{\,2} - \epsilon_d} \right\} \frac{1}{p''^{\,2}/m - \epsilon_d} \qquad (200)$$

２重の特異点は、部分分数法で避けられる。

One can avoid from the double singularities by the separation scheme.

特異点(2):Singularities

- Energy Complex Method
  Prog. Theor. Phys. 109 (2003) 869.

1. Sampling calculations with $E=E_{Real}+i\varepsilon$ where ε is tiny positive value.
2. Because of ε the calculaion can avoid from the singularities, but we need its stability.
3. Using these sampled data we get the solution of $\varepsilon=0$ by analytic comtinuation.

インプット:Input

- ２体力：Nucleon-Nucleon Force

ＡＶ１８，ＣＤＢｏｎｎ、ＮｉｊｍｅｇｅｎI，II

カイラル摂動ポテンシャル：ΧＰＴ（ＮＮＮＬＯ）

Chiral effective field theoretical potential

- ３体力： 3-body force

中間子交換型　ＦＭ、ＴＭ、ＵｒｂａｎａIX

(meson exchange type)

カイラル摂動３体力（ＮＮＮＬＯ）

Chiral effective field theoretical 3NF

Where to look for large 3NF effects? (PRL 81, 1183 (1998))

微分断面積:differential cross section

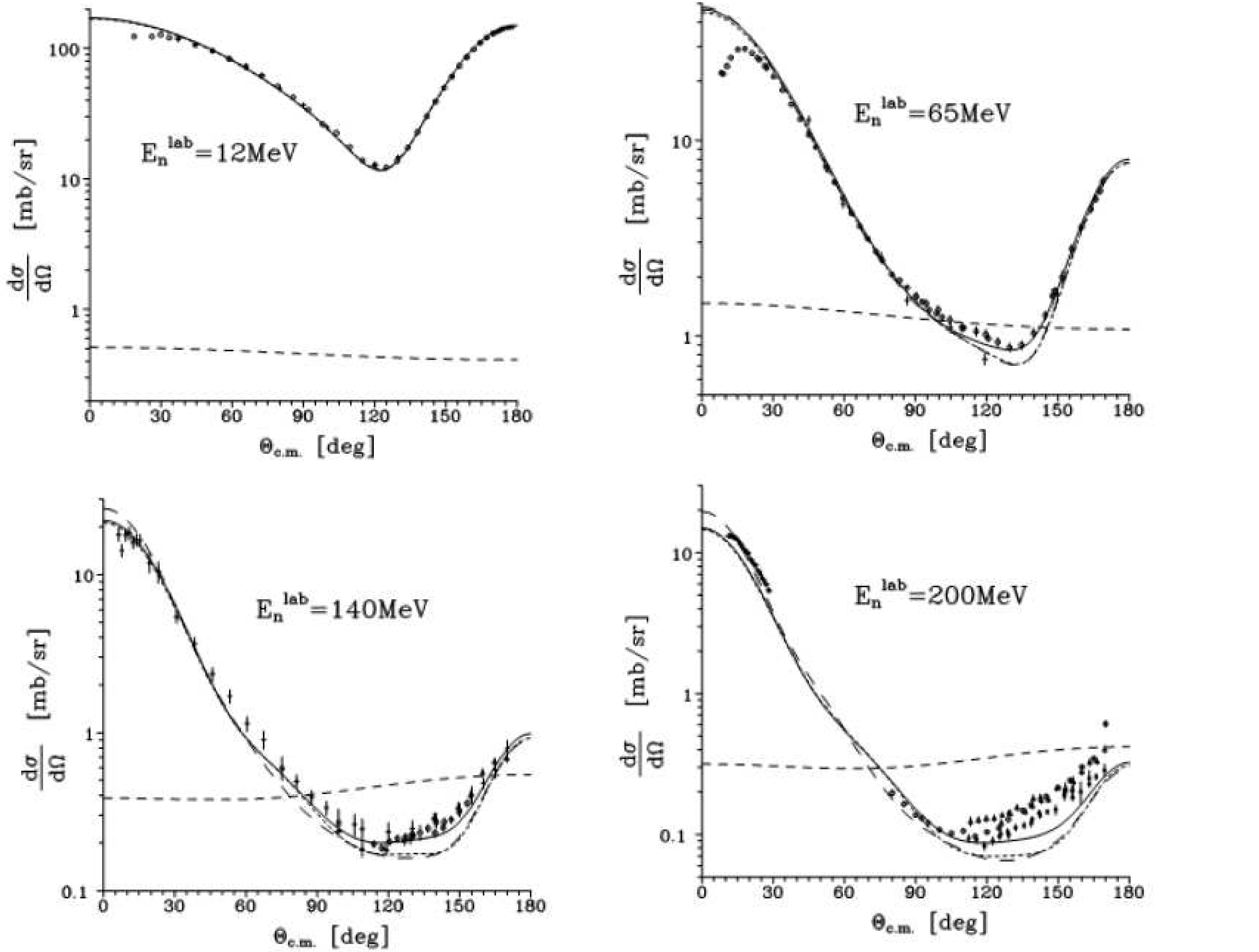

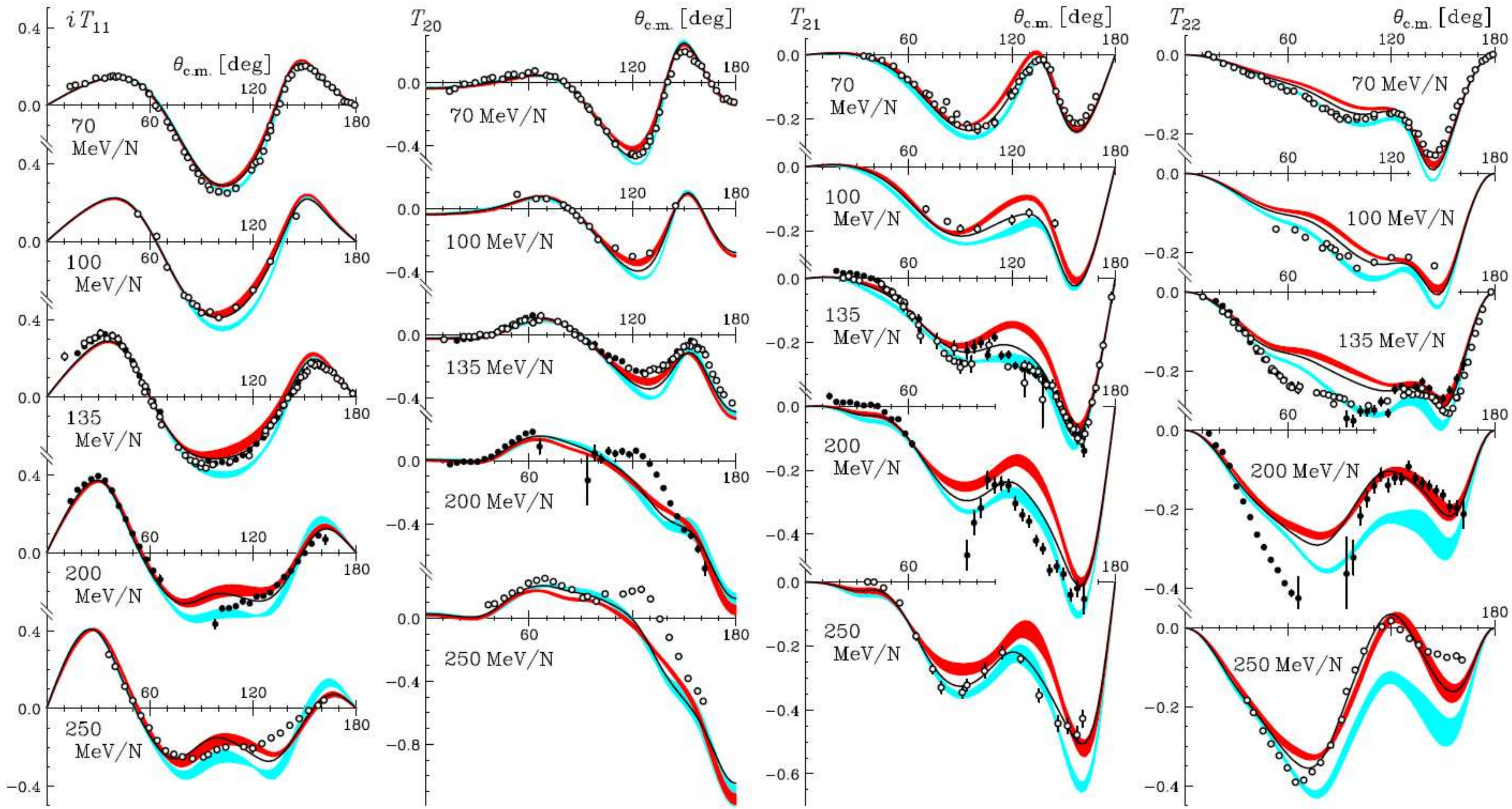

FIG. 1: (Color online) The deuteron analyzing powers iT_{11}, T_{20}, T_{21}, and T_{22} for dp elastic scattering at 70, 100, 135, 200, and 250 MeV/N. The light shaded (blue) bands contain predictions of modern NN potentials: AV18, CD Bonn, Nijmegen I and II. The dark shaded (red) bands result when those potentials are combined with TM99 3NF, properly adjusted to reproduce the ^{3}H binding energy. The solid line is the result obtained with the combination AV18+UIX. The pd data are: at 70 MeV/N (open circles) from Ref. [24], at 100 MeV/N (open circles) from Ref. [16], at 135 MeV/N (open circles) from Ref. [16] and (solid circles) from Ref. [23], at 200 MeV/N (solid circles) from Ref. [23], and at 250 MeV/N (open circles) from the present study.

K. Sekiguchi, et al., Physical Review C **83**, 061001(R) (2011)

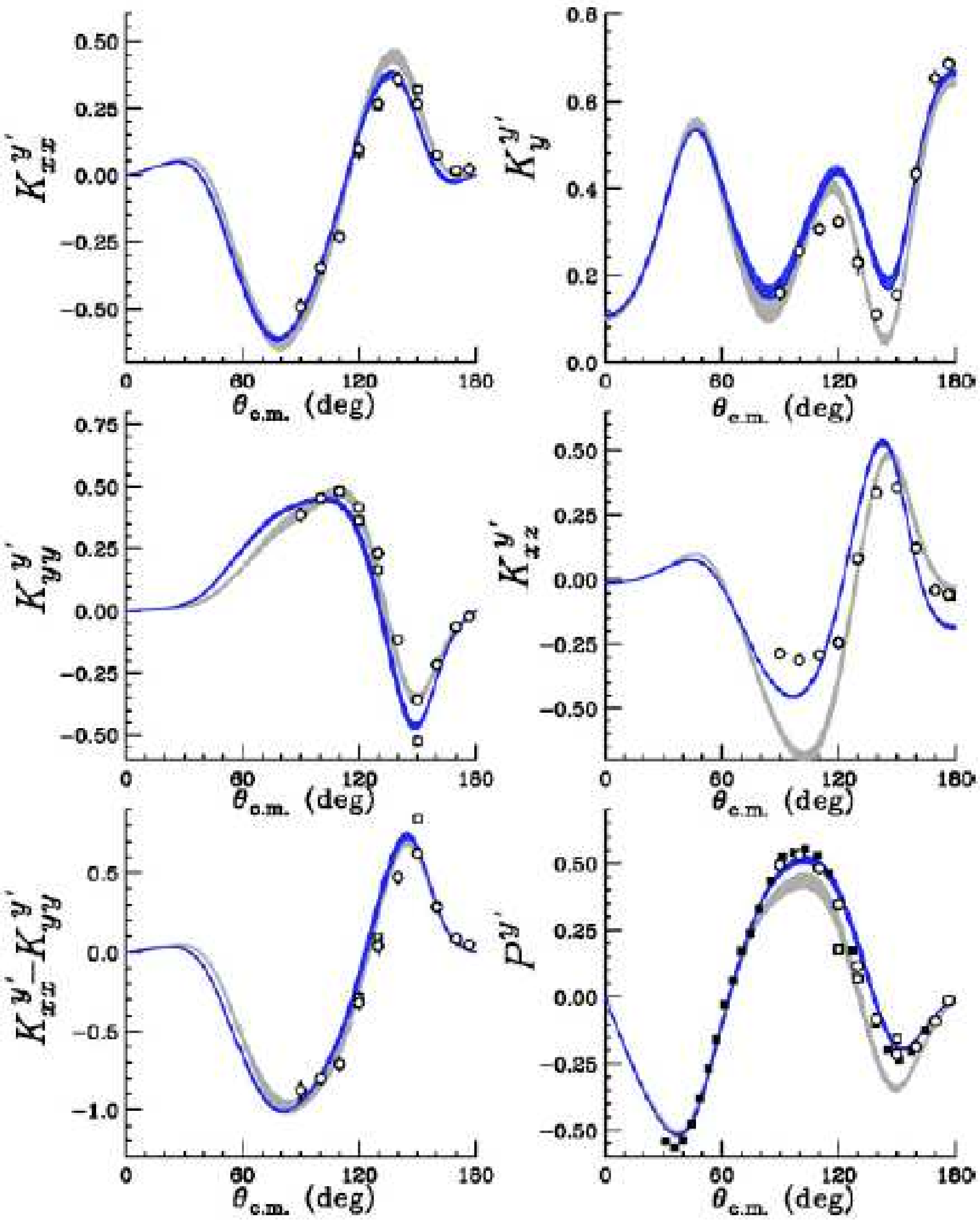

Polarization-transfer coefficients

FIG. 7. (Color online) polarization-transfer coefficients $K_{xx}^{y'}$, $K_{yy}^{y'}$, $K_{xx}^{y'}-K_{yy}^{y'}$, $K_{y}^{y'}$, $K_{xz}^{y'}$, and the induced polarization $P^{y'}$ in elastic d-p scattering at 135 MeV/nucleon. The light shaded bands contain the combinations of the NN + TM force predictions while the dark shaded bands include the combinations with TM′(99). For the descriptions of symbols, see Fig. 6.

Total cross section of pd scattering

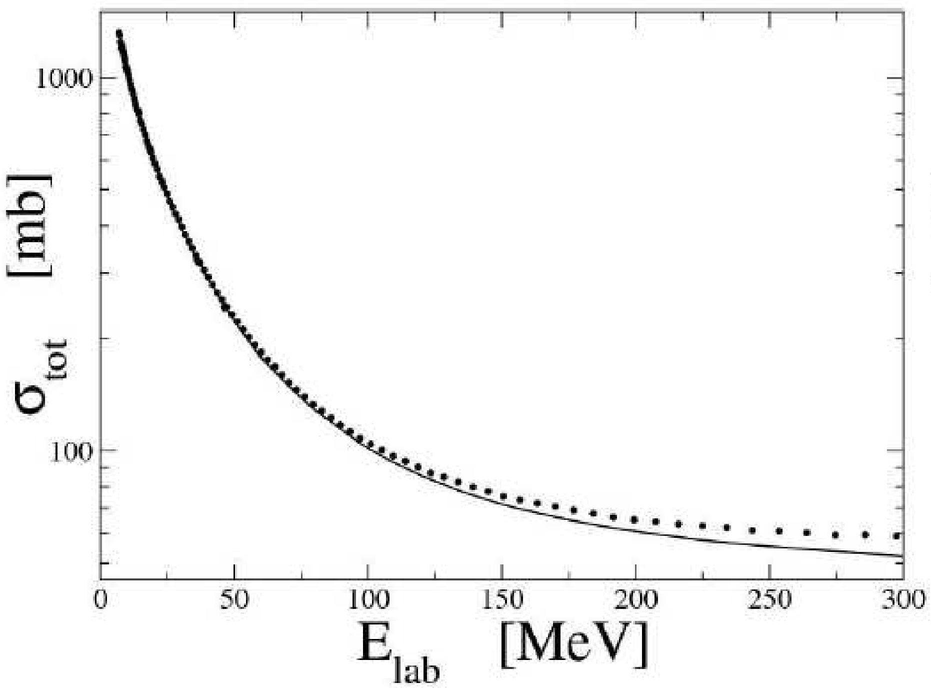

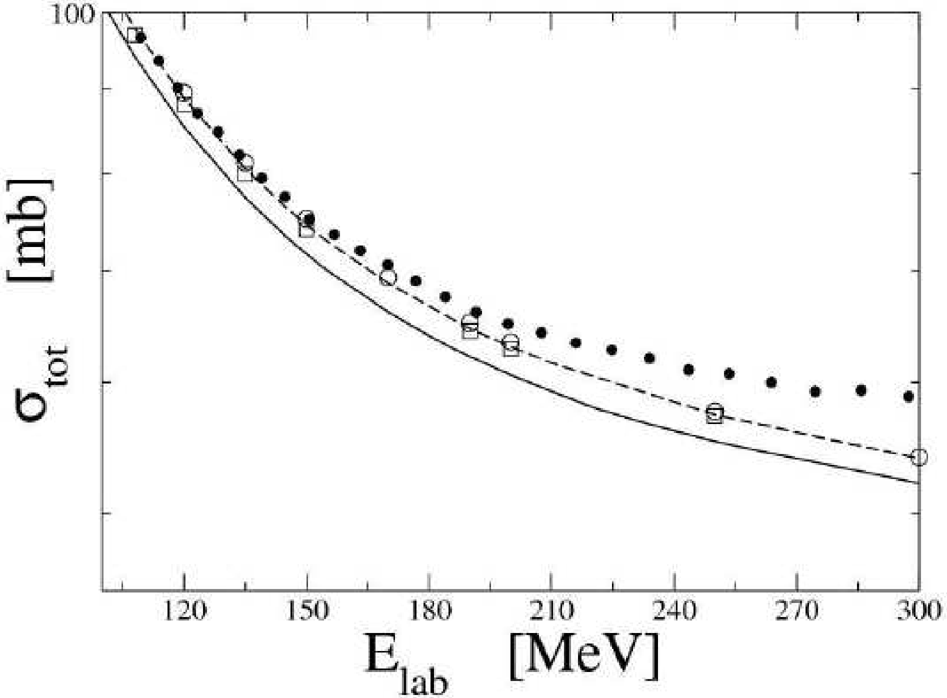

It is not enough to include the 3NF in the high energies.

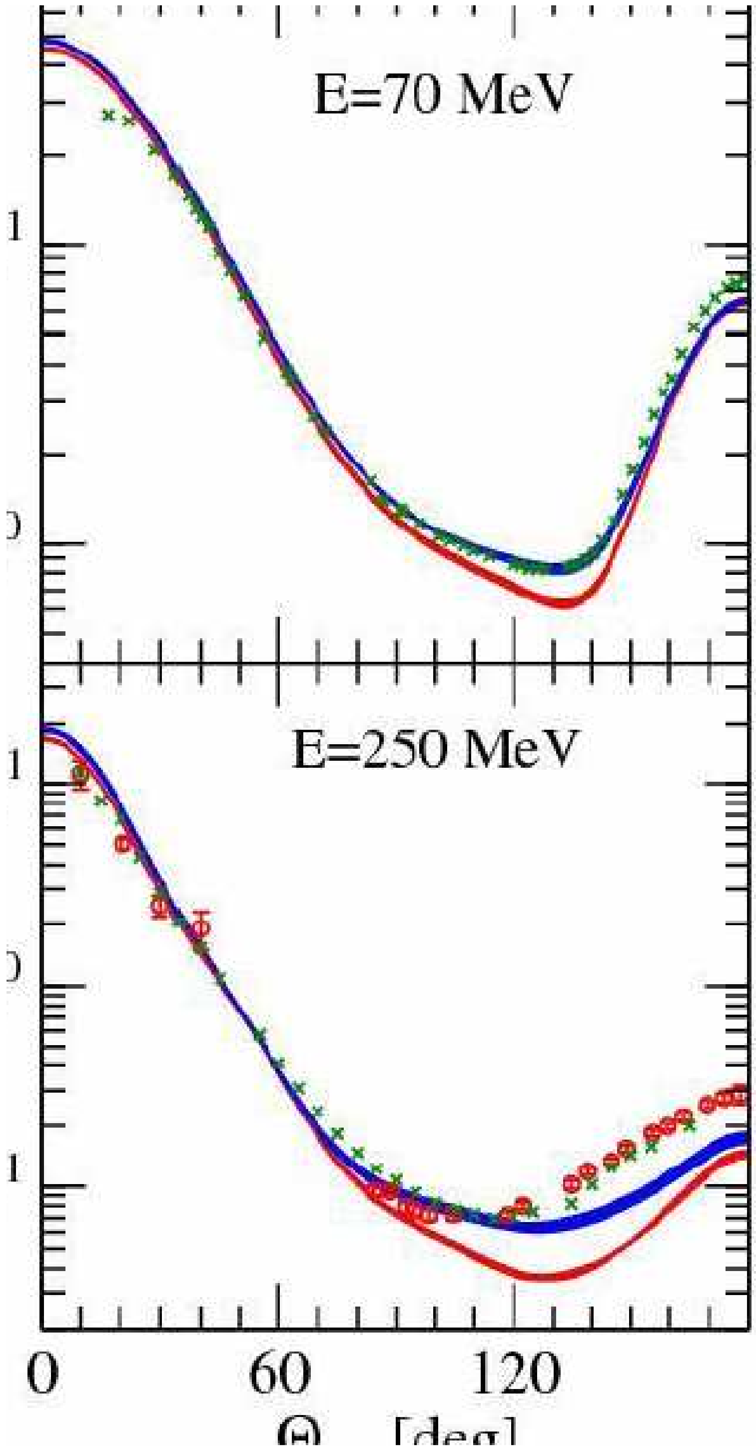

NN only (AV18, CD Bonn, Nijm1, N

NN+3NF TM99

70 MeV - RIKEN pd data
250 MeV – RCNP pd and nd data

カイラル有効場理論の３体力
3-body force in chiral effective field theory

- LO version→なし。No existence
- NLO version→なし。No exstence
- NNLO version→３つのタイプ。There are 3 types; Fujita-Miyazawa type, E-, D-type
- NNNLO→色々。;Many types

但し、新しいパラメータは導入しなくてもよい

One needs not to introduce new parameters (parameter free).

Few-nucleon forces in chiral EFT

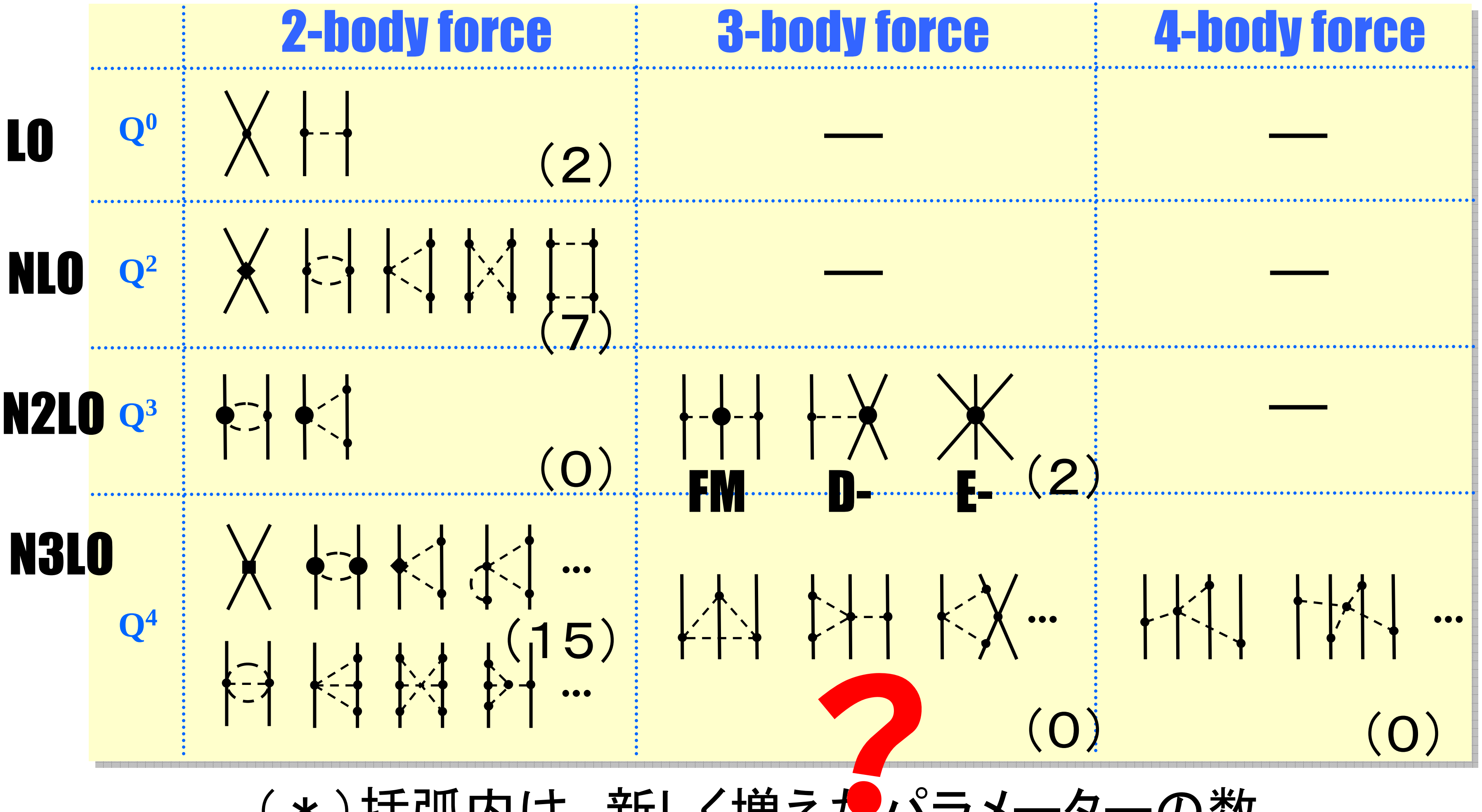

（＊）括弧内は、新しく増えたパラメーターの数

The number in the bracket means new increasing parameters.

Ptolemaic system

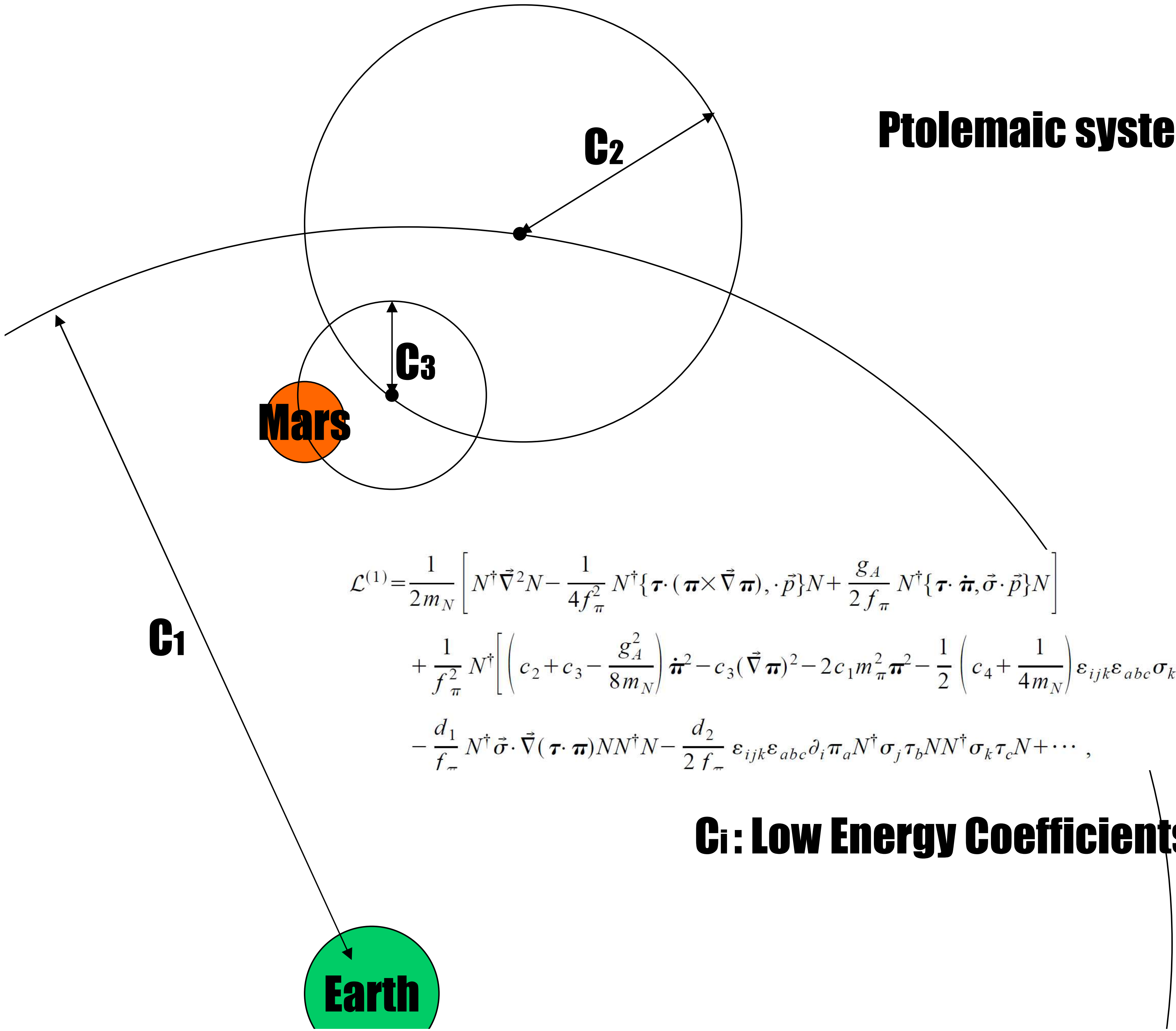

$$
\begin{aligned}
\mathcal{L}^{(1)} = {} & \frac{1}{2m_N}\left[N^\dagger \vec{\nabla}^2 N - \frac{1}{4f_\pi^2} N^\dagger\{\boldsymbol{\tau}\cdot(\boldsymbol{\pi}\times\vec{\nabla}\boldsymbol{\pi}), \cdot\vec{p}\}N + \frac{g_A}{2f_\pi} N^\dagger\{\boldsymbol{\tau}\cdot\dot{\boldsymbol{\pi}}, \vec{\sigma}\cdot\vec{p}\}N\right] \\
& + \frac{1}{f_\pi^2} N^\dagger\left[\left(c_2 + c_3 - \frac{g_A^2}{8m_N}\right)\dot{\boldsymbol{\pi}}^2 - c_3(\vec{\nabla}\boldsymbol{\pi})^2 - 2c_1 m_\pi^2 \boldsymbol{\pi}^2 - \frac{1}{2}\left(c_4 + \frac{1}{4m_N}\right)\varepsilon_{ijk}\varepsilon_{abc}\sigma_k\tau_c\partial_i\pi_a\partial_j\pi_b\right]N \\
& - \frac{d_1}{f_\pi} N^\dagger\vec{\sigma}\cdot\vec{\nabla}(\boldsymbol{\tau}\cdot\boldsymbol{\pi})NN^\dagger N - \frac{d_2}{2f_\pi}\varepsilon_{ijk}\varepsilon_{abc}\partial_i\pi_a N^\dagger\sigma_j\tau_b NN^\dagger\sigma_k\tau_c N + \cdots ,
\end{aligned}
$$

C_i : Low Energy Coefficients

The structure of the 3NF at N²LO

Forschungszentrum Jülich
in der Helmholtz-Gemeinschaft

- The explicit form of the 3NF was derived by van Kolck (PRC 49,2932)
  It turns out that the originally found 6 terms can be reduced to 3 using the antisymmetry of 3N states

FM

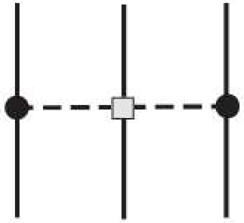

$$V^{2\pi}_{3NF} = \sum_{i<j<k} \left(\frac{g_A}{2F_\pi}\right)^2 \frac{\vec{\sigma}_i \cdot \vec{q}_i \ \vec{\sigma}_j \cdot \vec{q}_j}{(\vec{q}_i^{\,2} + m_\pi^2)(\vec{q}_j^{\,2} + m_\pi^2)} F^{\alpha\beta}_{ijk} \ \tau_i^\alpha \ \tau_j^\beta$$

$$F^{\alpha\beta}_{ijk} = \delta_{\alpha\beta}\left[-\frac{4c_1 m_\pi^2}{F_\pi^2} + \frac{2c_3}{F_\pi^2}\vec{q}_i \cdot \vec{q}_j\right] + \frac{c_4}{F_\pi^2}\epsilon^{\alpha\beta\gamma} \ \tau_k^\gamma \vec{\sigma}_k \cdot [\vec{q}_i \times \vec{q}_j]$$

a-term **b-term** **d-term**

D-

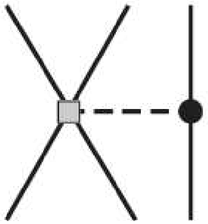

$$V^{1\pi}_{3NF} = -\sum_{i<j<k} \frac{g_A}{4F_\pi^2} \frac{c_D}{F_\pi^2 \Lambda_x} \frac{\vec{\sigma}_j \cdot \vec{q}_j}{\vec{q}_j^{\,2} + m_\pi^2} \ \tau_i \cdot \tau_j \ \vec{\sigma}_i \cdot \vec{\sigma}_j$$

E-

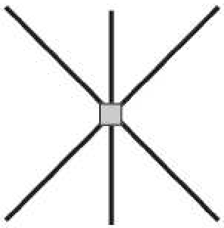

$$V^{c}_{3NF} = \sum_{i<j<k} \frac{c_E}{F_\pi^4 \Lambda_x} \ \tau_j \cdot \tau_k$$

稼動中
Available

- c_i are related to πN scattering and also the NN force (consistency to NN force!)

- c_D and c_E can be determined from the 3N and 4N systems

２００６．１１．１７

The structure of the 3NF at N^{3}LO

(with Bernard & Meißner, work in progress)

部分波展開終了
プログラム化中
In progress

2π – exchange

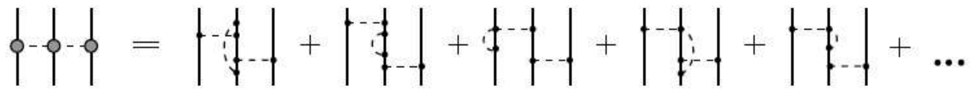

$\in$ Fujita-Miyazawa, TM and Urbana

2π-1π – exchange

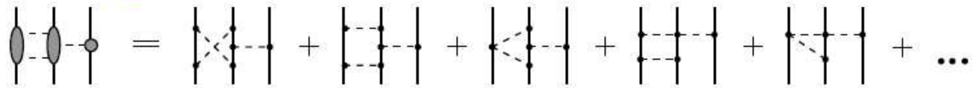

$\in$ Canton-Schadow

2π – exchange between all three nucleons

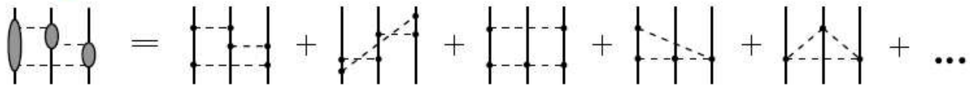

$\in$ Illinoi 3NF

T=3/2で重要といわれている。

稼動中
available

ntact-1π – exchange

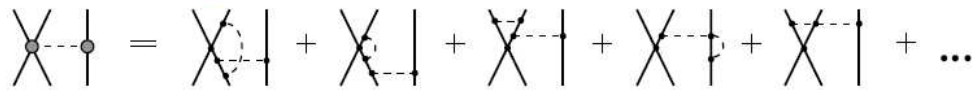

$\in$ Hueber

D- {

contact-2π – exchange

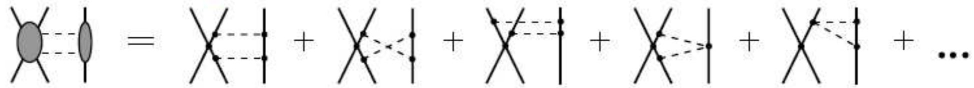

+ $1/m$ - corrections

no new 3N contact interactions $\Longrightarrow$ parameter-free!

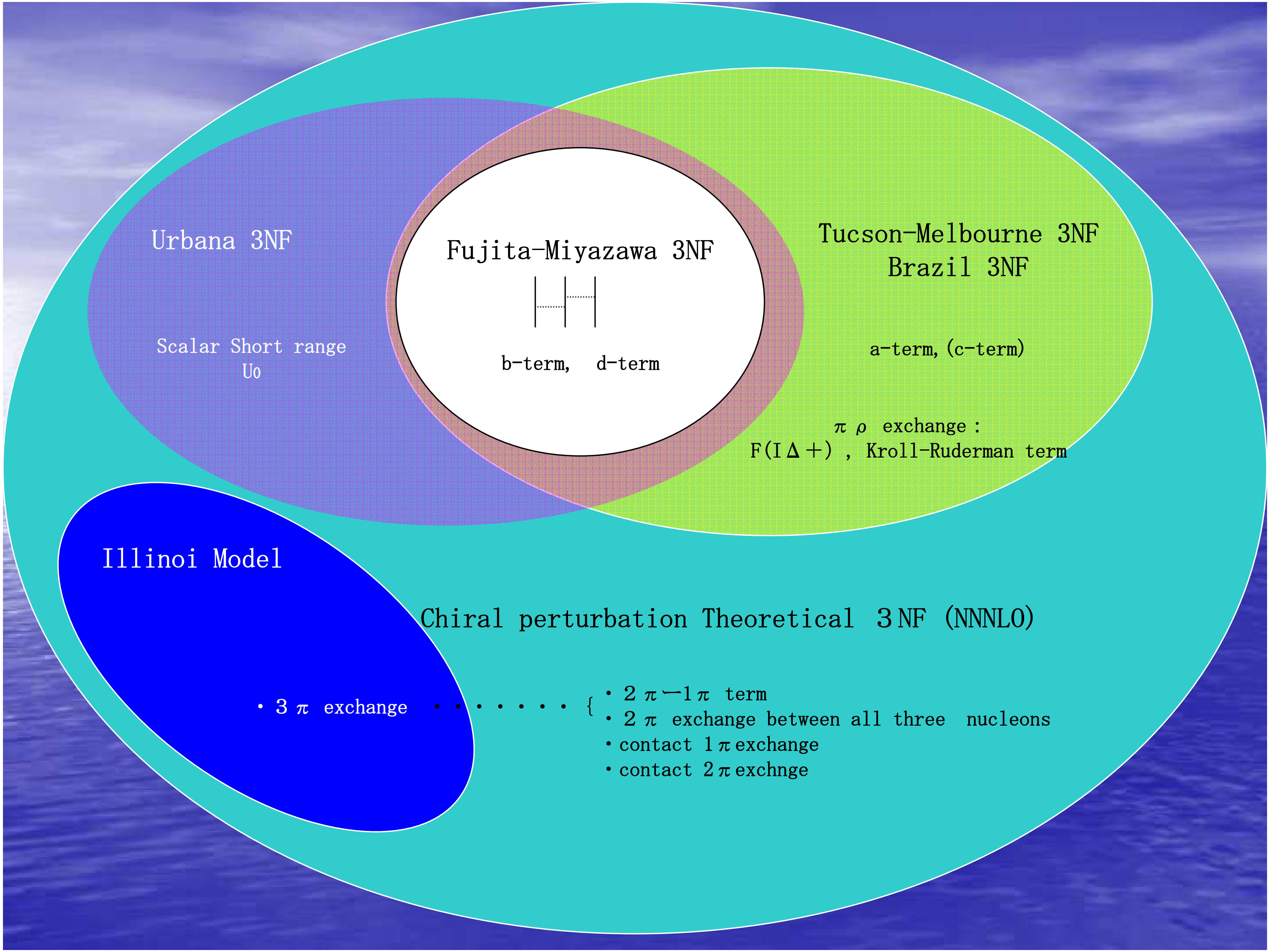

Urbana 3NF
Scalar Short range
U0
Fujita-Miyazawa 3NF
b-term, d-term
Tucson-Melbourne 3NF
Brazil 3NF
a-term, (c-term)
π ρ exchange :
F(IΔ+) , Kroll-Ruderman term
Illinoi Model
Chiral perturbation Theoretical 3NF (NNNLO)
・3π exchange ・・・・・・・{
・2π−1π term
・2π exchange between all three nucleons
・contact 1π exchange
・contact 2π exchnge

カイラル有効場ポテンシャルの結果
Some results from Chiral FT pot.

- NLO
- NNLO
- NNNO （News　1）

Elastic nucleon-deuteron scattering observables

E=3 MeV

E=10 MeV

E=65 MeV

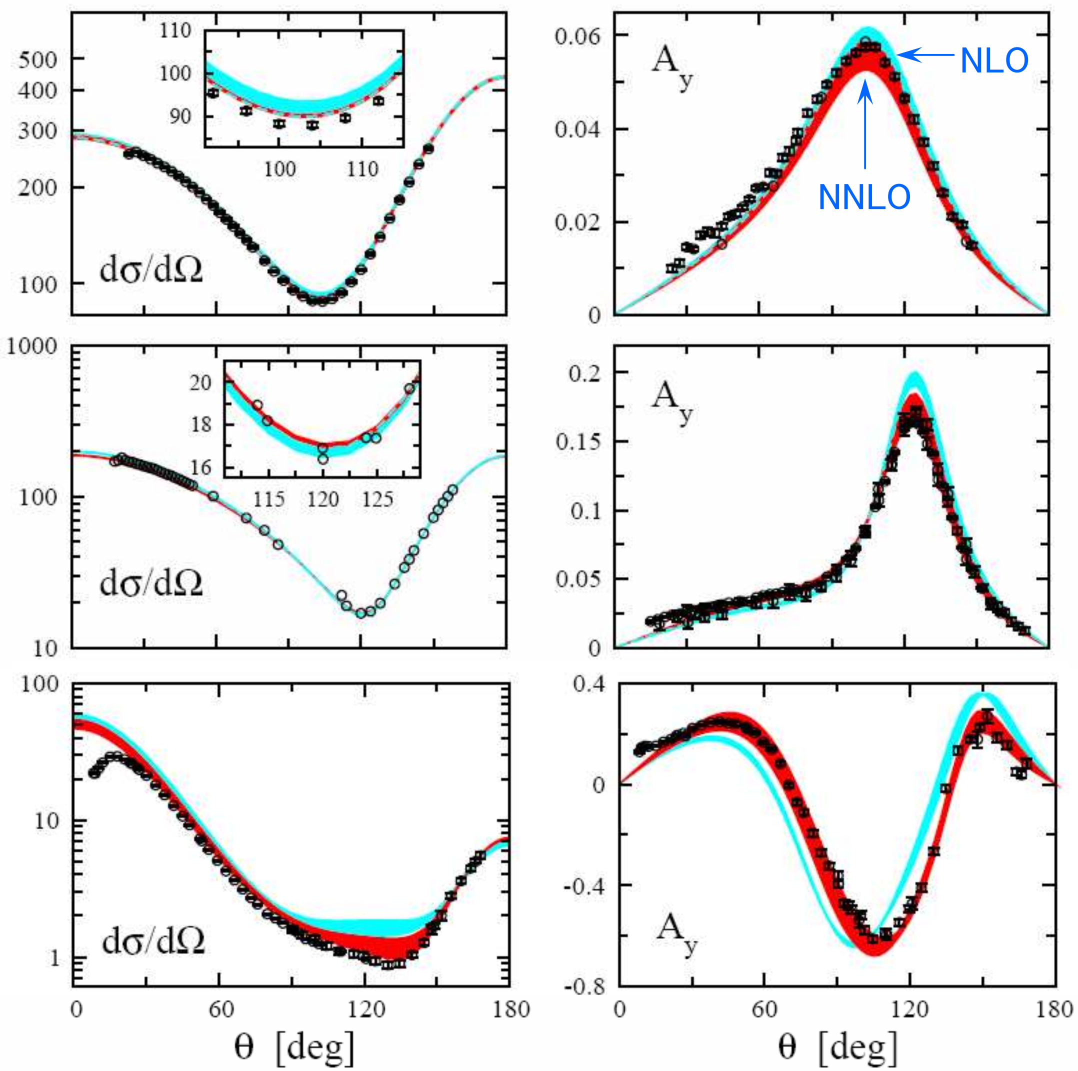

nd + Coulomb-corrected pd data

Polarization transfer coefficients in $d(\vec{p}, \vec{p})d$ and $d(\vec{p}, \vec{d})p$ at E_p=22.7 MeV

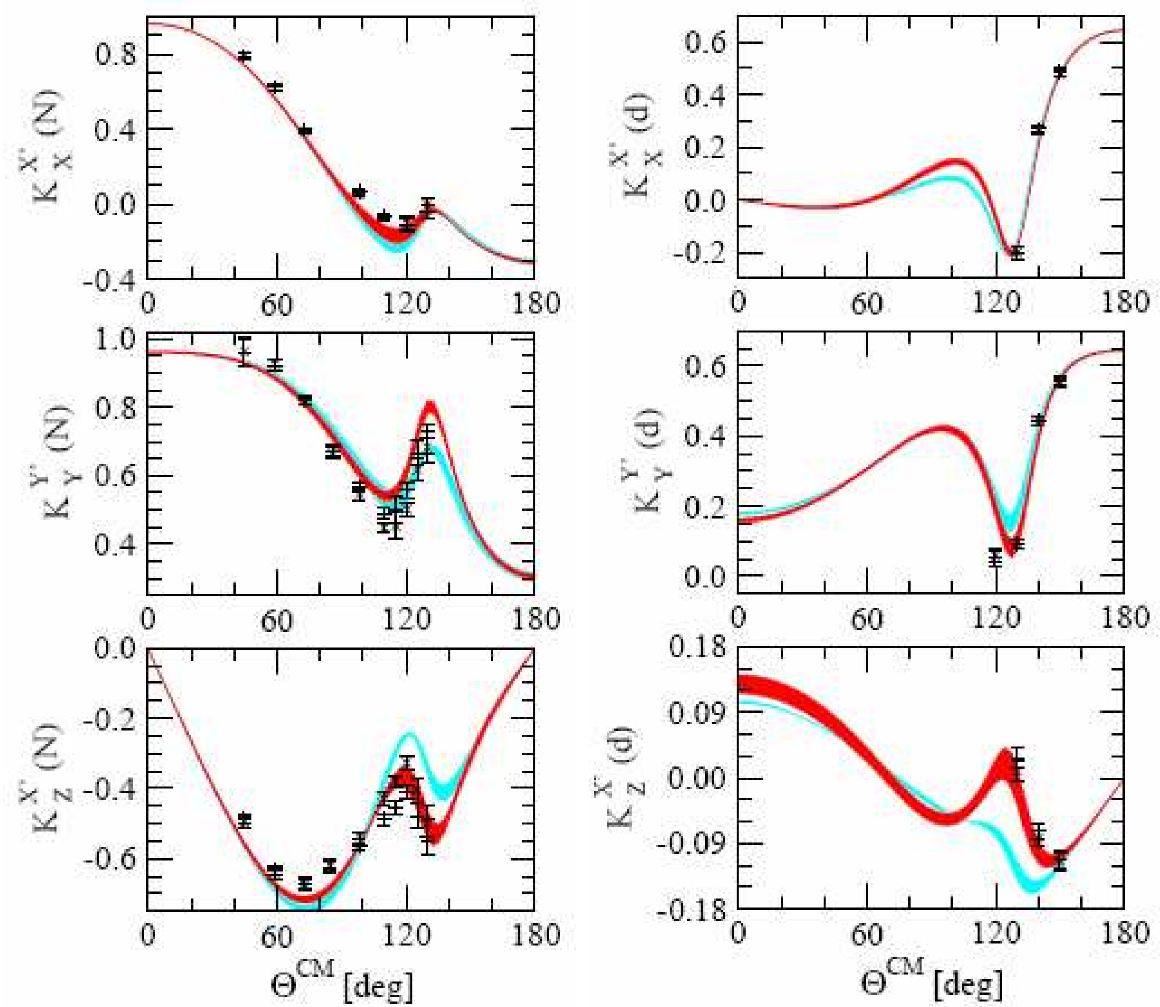

Coulomb-corrected pd data

H. Witała et al., PRC 73 (2006) 044004

Breakup cross section in the reaction $d(p, pp)n$ at E_p=16 MeV

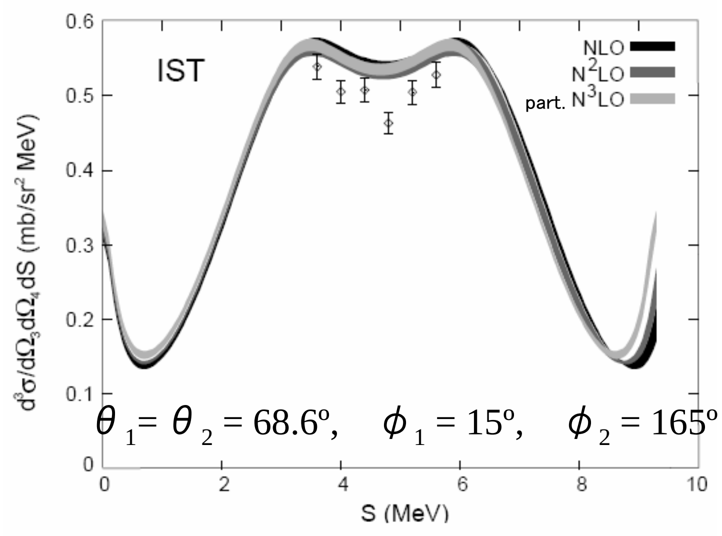

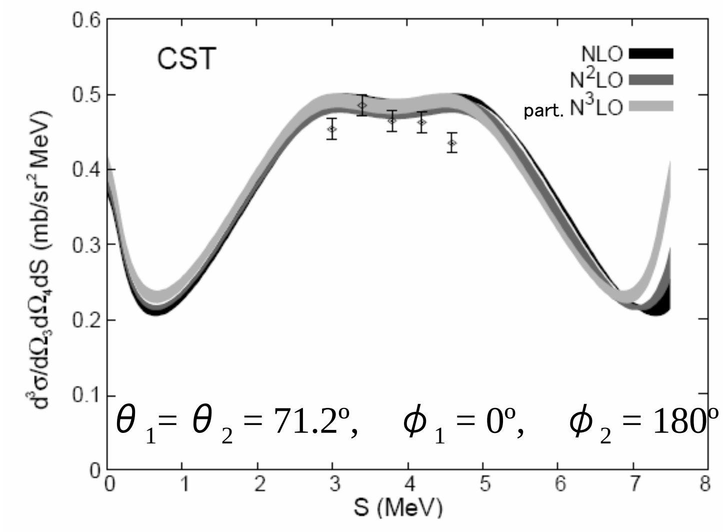

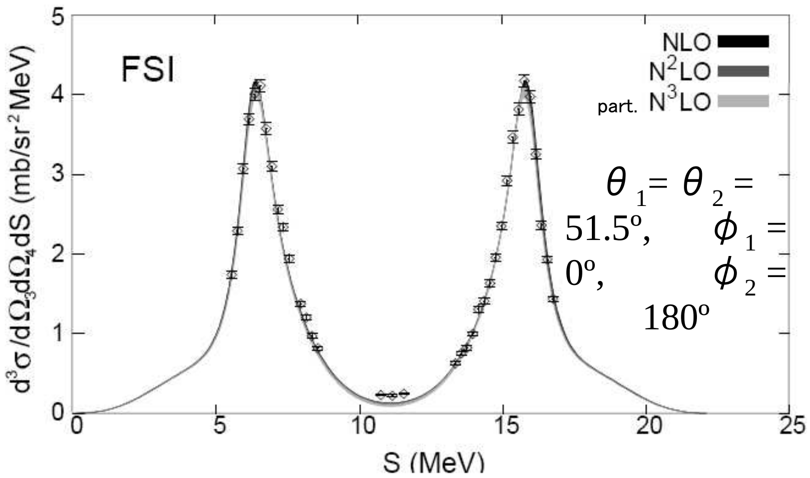

C. Düwecke et al., PRC 72 (2006) 044001

Some open problems…

Deuteron breakup in the Symmetric Constant Relative Energy (SCRE) configuration at E_d=19 MeV

Ley et al., PRC 73 (2006) 064001

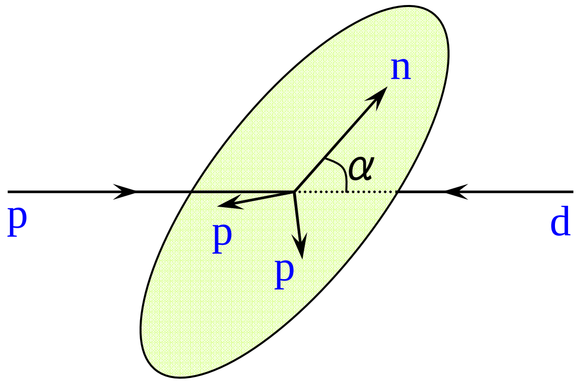

Differential cross section

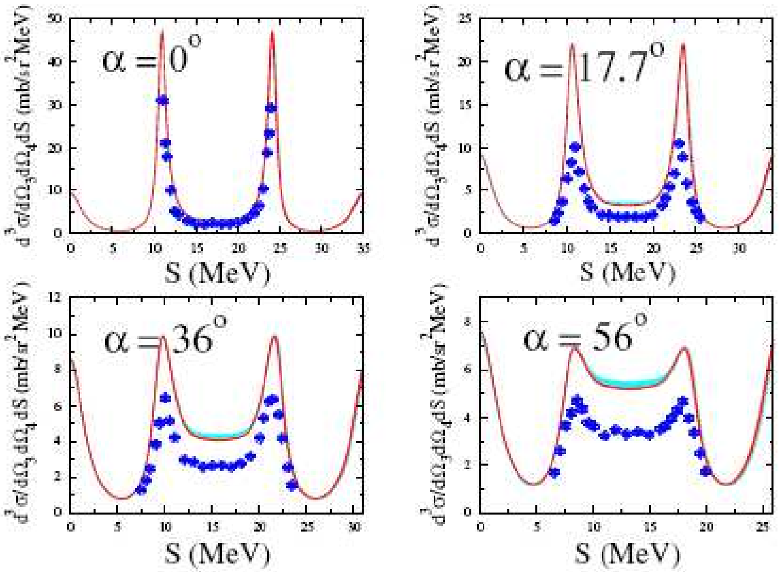

Tensor analyzing power A_{yy}

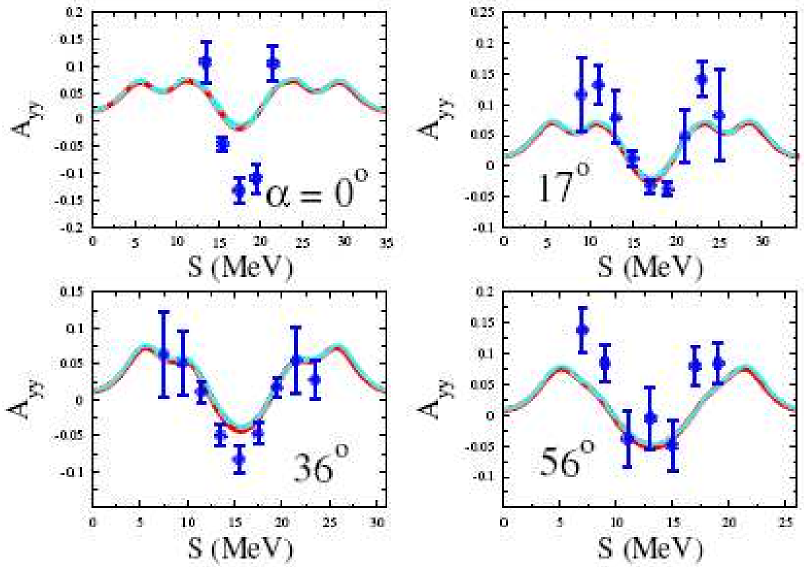

<u>Notice</u>: including Coulomb interaction reduces the discrepancy for the cross section by about 30% and improves the description of A_{yy}

More nucleons...

α-particle

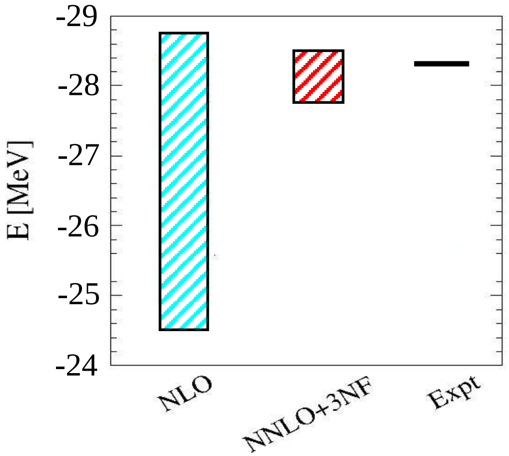

^{6}Li ground and excited states

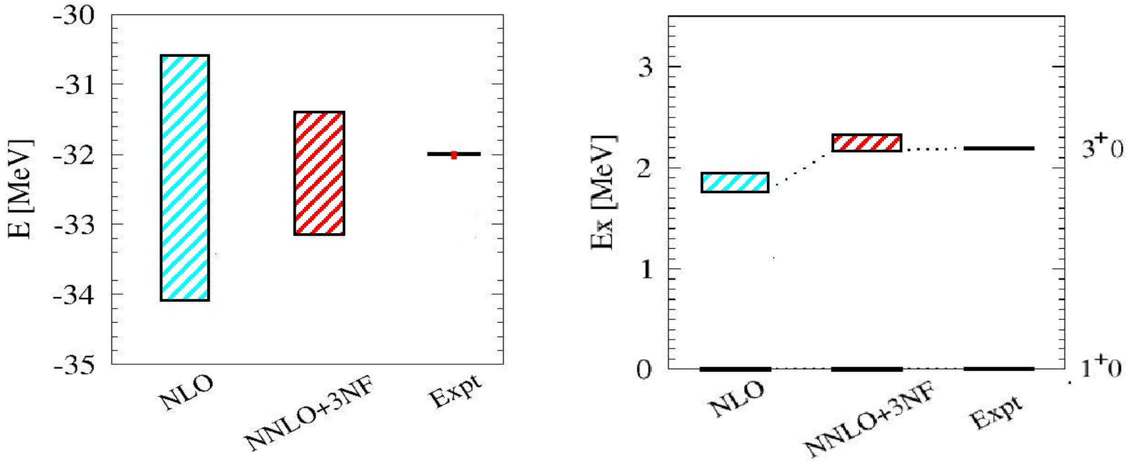

calculated by Andreas Nogga

Calculations based on chiral forces up to A=13 carried out by *Navratil et al. '06,'07*

It is very important to go to N^{3}LO to further test chiral EFT in the few-nucleon sector and to see whether the remaining problems can be solved!

problems

- **what is responsible for large differences between theory and data in 250 MeV cross section even after inclusion of 2π-exchange 3NF ?**

- **how to explain the complex pattern of differences between data and theory for spin observables ?**

- **it is evident, that in the applied dynamics something is wrong or missing**

- **χPT (and standard meson-exchange picture) provides multitude of additional, short-range components to 3NF (in the meson-exchange picture connected to exchanges of more or heavier mesons), which should be more important with increasing energy**

- **however, increasing energy means also a transition to a region, where relativity could be important**

展望:Hope

D-type, E-type of 3NF (NNLO) may solve the Sagara-discrepancy at high energy (>200MeV).

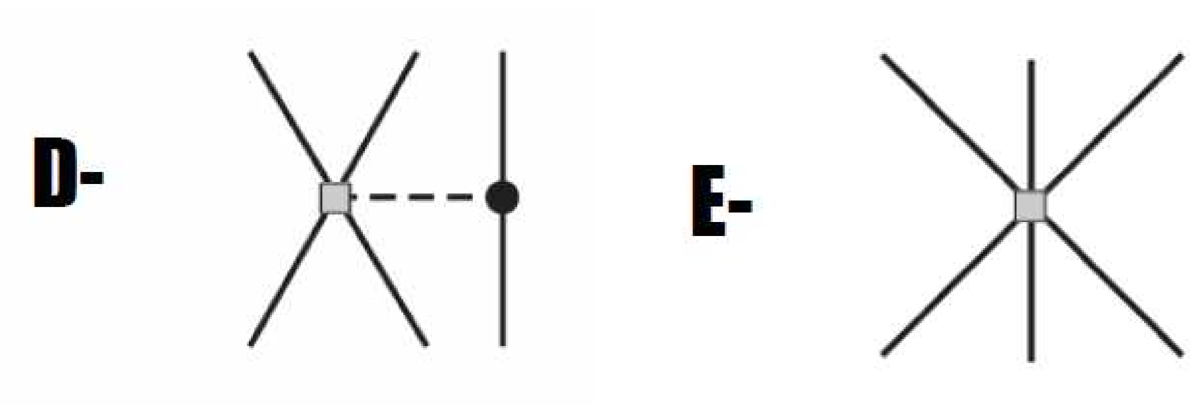

News 1

- Automitized Partial Wave Decomposition (aPWD) is developed using Mathematica. The aPWD writes FORTRAN codes.

Eur. Phys. J. A (2011) **47**,48; **arXiv:1101.2150 [nucl-th].**

- Calibration of the code by comparing the former scheme with π ρ exchange 3NF.

- 3NFof NNNLO version is prepared to calculate the binding energy of Triton.

arXiv:1107.5163

arXiv:1107.5163v1 [nucl-th] 26 Jul 2011

$$V_{2\pi}^{(1)} = F_1\, \vec{\sigma_2} \cdot \vec{q_2}\, \vec{\sigma_3} \cdot \vec{q_3}\, \boldsymbol{\tau_2} \cdot \boldsymbol{\tau_3} + F_2\, \vec{\sigma_2} \cdot \vec{q_2}\, \vec{\sigma_3} \cdot \vec{q_3}\, \vec{q_2} \times \vec{q_3} \cdot \vec{\sigma_1}\, \boldsymbol{\tau_2} \times \boldsymbol{\tau_3} \cdot \boldsymbol{\tau_1}$$

$$c_1 = -0.81\ \mathrm{GeV}^{-1}, \qquad c_3 = -3.40\ \mathrm{GeV}^{-1}, \qquad c_4 = 3.40\ \mathrm{GeV}^{-1}\,.$$

$$\begin{aligned} V_{2\pi-1\pi}^{(1)} &= \frac{\vec{\sigma}_1 \cdot \vec{q}_1}{q_1^2 + M_\pi^2} \Big[\boldsymbol{\tau}_2 \cdot \boldsymbol{\tau}_1 \; (\vec{\sigma}_3 \cdot \vec{q}_2\, \vec{q}_2 \cdot \vec{q}_1\; F_1(q_2) + \vec{\sigma}_3 \cdot \vec{q}_2\; F_2(q_2) + \vec{\sigma}_3 \cdot \vec{q}_1\; F_3(q_2)) \\ &+ \boldsymbol{\tau}_3 \cdot \boldsymbol{\tau}_1\; (\vec{\sigma}_2 \cdot \vec{q}_2\, \vec{q}_2 \cdot \vec{q}_1\; F_4(q_2) + \vec{\sigma}_2 \cdot \vec{q}_1\; F_5(q_2) + \vec{\sigma}_3 \cdot \vec{q}_2\; F_6(q_2) + \vec{\sigma}_3 \cdot \vec{q}_1\; F_7(q_2)) \\ &+ \boldsymbol{\tau}_2 \times \boldsymbol{\tau}_3 \cdot \boldsymbol{\tau}_1\; \vec{\sigma}_2 \times \vec{\sigma}_3 \cdot \vec{q}_2\; F_8(q_2) \Big] + (2 \leftrightarrow 3)\,. \qquad (2.1 \end{aligned}$$

$$\begin{aligned} V_{ring}^{(1)} &= \vec{\sigma}_1 \cdot \vec{\sigma}_2\, \boldsymbol{\tau}_2 \cdot \boldsymbol{\tau}_3\, R_1 + \vec{\sigma}_1 \cdot \vec{q}_1 \vec{\sigma}_2 \cdot \vec{q}_1\, \boldsymbol{\tau}_2 \cdot \boldsymbol{\tau}_3\, R_2 + \vec{\sigma}_1 \cdot \vec{q}_1 \vec{\sigma}_2 \cdot \vec{q}_3\, \boldsymbol{\tau}_2 \cdot \boldsymbol{\tau}_3\, R_3 \\ &+ \vec{\sigma}_1 \cdot \vec{q}_3 \vec{\sigma}_2 \cdot \vec{q}_1\, \boldsymbol{\tau}_2 \cdot \boldsymbol{\tau}_3\, R_4 + \vec{\sigma}_1 \cdot \vec{q}_3 \vec{\sigma}_2 \cdot \vec{q}_3\, \boldsymbol{\tau}_2 \cdot \boldsymbol{\tau}_3\, R_5 + \boldsymbol{\tau}_1 \cdot \boldsymbol{\tau}_3\, R_6 + \vec{\sigma}_1 \cdot \vec{q}_1 \vec{\sigma}_3 \cdot \vec{q}_1\, R_7 \\ &+ \vec{\sigma}_1 \cdot \vec{q}_1 \vec{\sigma}_3 \cdot \vec{q}_3\, R_8 + \vec{\sigma}_1 \cdot \vec{q}_3 \vec{\sigma}_3 \cdot \vec{q}_1\, R_9 + \vec{\sigma}_1 \cdot \vec{\sigma}_3\, R_{10} + \vec{q}_1 \cdot \vec{q}_3 \times \vec{\sigma}_2\, \boldsymbol{\tau}_1 \cdot \boldsymbol{\tau}_2 \times \boldsymbol{\tau}_3\, R_{11} \\ &+ \boldsymbol{\tau}_1 \cdot \boldsymbol{\tau}_2\, S_1 + \vec{\sigma}_1 \cdot \vec{q}_1 \vec{\sigma}_3 \cdot \vec{q}_1\, \boldsymbol{\tau}_1 \cdot \boldsymbol{\tau}_2\, S_2 + \vec{\sigma}_1 \cdot \vec{q}_3 \vec{\sigma}_3 \cdot \vec{q}_1\, \boldsymbol{\tau}_1 \cdot \boldsymbol{\tau}_2\, S_3 + \vec{\sigma}_1 \cdot \vec{q}_1 \vec{\sigma}_3 \cdot \vec{q}_3\, \boldsymbol{\tau}_1 \cdot \boldsymbol{\tau}_2\, S_4 \\ &+ \vec{\sigma}_1 \cdot \vec{q}_3 \vec{\sigma}_3 \cdot \vec{q}_3\, \boldsymbol{\tau}_1 \cdot \boldsymbol{\tau}_2\, S_5 + \vec{\sigma}_1 \cdot \vec{\sigma}_3\, \boldsymbol{\tau}_1 \cdot \boldsymbol{\tau}_2\, S_6 + \vec{q}_1 \cdot \vec{q}_3 \times \vec{\sigma}_1\, \boldsymbol{\tau}_1 \cdot \boldsymbol{\tau}_2 \times \boldsymbol{\tau}_3\, S_7 \\ &+ (2 \leftrightarrow 3)\,, \qquad (2.11) \end{aligned}$$

$$
\begin{aligned}
F_1 &= \frac{g_A^4}{4F_\pi^4}\,\frac{(-4\tilde{c}_1 M_\pi^2 + 2\tilde{c}_3 \vec{q_2}\cdot\vec{q_3})}{(q_2^2+M_\pi^2)(q_3^2+M_\pi^2)} + \tilde{F}_1 \\
F_2 &= \frac{g_A^4}{4F_\pi^4}\,\frac{\tilde{c}_4}{(q_2^2+M_\pi^2)(q_3^2+M_\pi^2)} + \tilde{F}_2 \, ,
\end{aligned}
$$

with

$$
\begin{aligned}
\tilde{F}_1 &= \frac{g_A^4}{128\pi F_\pi^6}\frac{1}{(q_2^2+M_\pi^2)(q_3^2+M_\pi^2)}(M_\pi(M_\pi^2+3q_2^2+3q_3^2+4\vec{q_2}\cdot\vec{q_3}) \\
&+ (2M_\pi^2+q_2^2+q_3^2+2\vec{q_2}\cdot\vec{q_3})(3M_\pi^2+3q_2^2+3q_3^2+4\vec{q_2}\cdot\vec{q_3})A(|\vec{q_2}+\vec{q_3}|)) \\
\tilde{F}_2 &= \frac{-g_A^4}{128\pi F_\pi^6}\frac{1}{(q_2^2+M_\pi^2)(q_3^2+M_\pi^2)}(M_\pi+(4M_\pi^2+q_2^2+q_3^2+2\vec{q_2}\cdot\vec{q_3})A(|\vec{q_2}+\vec{q_3}|)) \, ,
\end{aligned}
$$

3体力の特有の新しいLEC：D，E

$$V^{(1)}_{d-term} = -\frac{g_A D}{8F_\pi^2} \frac{\vec{\sigma}_1 \cdot \vec{q}_1}{q_1^2 + M_\pi^2} \left(\boldsymbol{\tau}_1 \cdot \boldsymbol{\tau}_3 \, \vec{\sigma}_3 \cdot \vec{q}_1 + \boldsymbol{\tau}_1 \cdot \boldsymbol{\tau}_2 \, \vec{\sigma}_2 \cdot \vec{q}_1 \right) .$$

$$V^{(1)}_{e-term} = E \boldsymbol{\tau}_2 \cdot \boldsymbol{\tau}_3$$

$$D = c_D/(F_\pi^2 \Lambda_\chi), \quad E = c_E/(F_\pi^4 \Lambda_\chi)$$

$F_\pi = 92.4$ MeV for the pion decay constant

the chiral symmetry breaking scale Λ_χ is estimated to be $\Lambda_\chi = 700$ MeV.

cut-off	$(\Lambda, \tilde{\Lambda})$	c_D	c_E
1	(450,500)	10.78	-0.172
2	(600,500)	12.00	1.254
3	(550,600)	11.67	2.120
4	(450,700)	7.21	-0.748
5	(600,700)	14.07	1.704

cut-off	$\langle H_0 \rangle$ [MeV]	$\langle V_{NN} \rangle$ [MeV]	$\langle V_{3N} \rangle$ [MeV]
1	35.972	-43.459	-0.994
2	54.708	-61.515	-1.673
3	48.088	-55.187	-1.381
4	33.232	-41.050	-0.663
5	53.504	-60.278	-1.706

cut-off	$\langle V_{2\pi} \rangle$ [MeV]	$\langle V_{2\pi-1\pi} \rangle$ [MeV]	$\langle V_{ring} \rangle$ [MeV]	$\langle V_{d-term} \rangle$ [MeV]	$\langle V_{e-term} \rangle$ [MeV]
1	-0.639	0.458	-0.147	-0.693	0.027
2	-0.241	-0.580	-1.114	0.694	-0.432
3	-0.473	0.107	-0.191	-0.708	-0.116
4	-0.771	0.539	-0.452	-0.259	0.281
5	-0.377	-0.275	-0.622	-0.119	-0.313

相対論的3体計算:
Relativistic 3body calculation

- ローレンツ不変 ; Lorentz invariance
  相対論的量子力学
  Relativistic quantum mechanics
- (場の量子論への拡張)
  Field theoretical approach

  。。。

・Relativity

The nonrelativistic **theoretical prediction of the Nd scattering cross section beyond 200MeV/u is getting to be** poor **even including the 3-body force (FM type).**

What is missing?

Relativistic Calculation

There are essentially two different approaches to relativistic three-nucleon calculation:

① a manifestly covariant scheme linked to a field theoretical approach.

② a scheme based on relativistic quantum mechanics on spacelike hypersurfaces (including the light front) in Minkowski space.

B. Bakamjian, L.H. Thomas, Phys. Rev. 92, 1300 (1952).

- Within the second scheme the relativistic Hamiltonian for on-the-mass-shell particles consists of relativistic kinetic energies and two- and many-body interactions including their boost corrections, which are dictated by the Poincare algebra.

What is the boost correction?

A potential in an arbitrary moving frame (q≠0) is different, which enters a relativistic Lippmann-Schwinger equation.

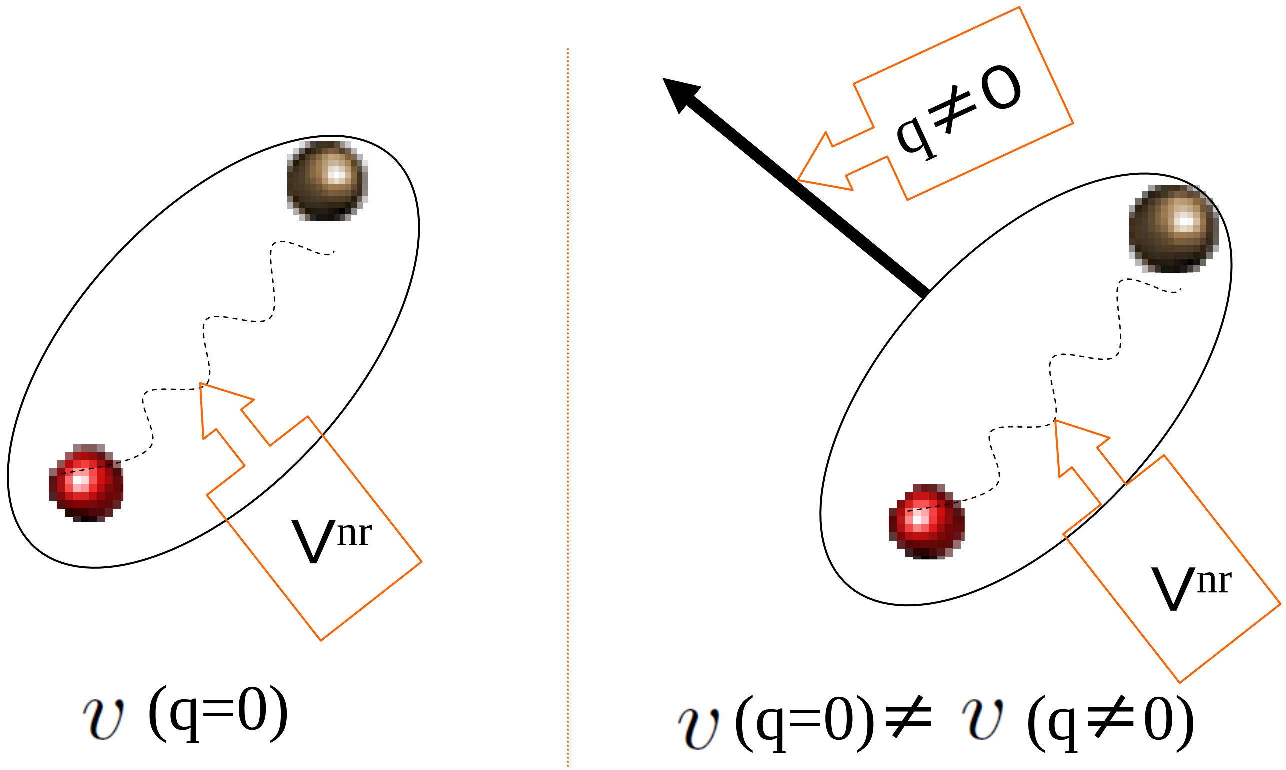

v (q=0) $\qquad$ v (q=0) ≠ v (q≠0)

Two-body t-matrix

Nonrelativistic LS eq.

$$\overset{nr}{t}(\vec{k},\vec{k}\,';\, E) = v^{nr}(\vec{k},\vec{k}\,') + \int d^3k'' \frac{v^{nr}(\vec{k},\vec{k}\,'')\,\overset{nr}{t}(\vec{k}\,'',\vec{k}\,';\, E)}{E - k''^2/m + i\epsilon}.$$

Relativistic LS eq.

$$\hat{t}(\vec{k},\vec{k}\,';\vec{q}\,) = v(\vec{k},\vec{k}\,') + \int d^3k'' \frac{v(\vec{k},\vec{k}\,'')\,\hat{t}(\vec{k}\,'',\vec{k}\,';\vec{q}\,)}{2\omega(\vec{k}\,') - 2\omega(\vec{k}\,'') + i\epsilon}.$$

Boosted relativisitic LS eq.

$$t(\vec{k},\vec{k}\,';\vec{q}\,) = V(\vec{k},\vec{k}\,';\vec{q}\,) + \int d^3k'' \frac{V(\vec{k},\vec{k}\,'';\vec{q}\,)\,t(\vec{k}\,'',\vec{k}\,';\vec{q}\,)}{\sqrt{(2\omega(\vec{k}\,'))^2 + \vec{q}^{\,2}} - \sqrt{(2\omega(\vec{k}\,''))^2 + \vec{q}^{\,2}} + i\epsilon}.$$

Two-body t-matrix

Nonrelativistic LS eq.

$$\overset{nr}{t}(\vec{k},\vec{k}\,';\ E) = v^{nr}(\vec{k},\vec{k}\,') + \int d^3k'' \frac{v^{nr}(\vec{k},\vec{k}\,'')\overset{nr}{t}(\vec{k}\,'',\vec{k}\,';\ E)}{E - k''^2/m + i\epsilon}.$$

Relativistic LS eq.

$$\hat{t}(\vec{k},\vec{k}\,';\vec{q}\,) = v(\vec{k},\vec{k}\,') + \int d^3k'' \frac{v(\vec{k},\vec{k}\,'')\hat{t}(\vec{k}\,'',\vec{k}\,';\vec{q}\,)}{2\omega(\vec{k}\,') - 2\omega(\vec{k}\,'') + i\epsilon}.$$

Boosted relativisitic LS eq.

$$t(\vec{k},\vec{k}\,';\vec{q}\,) = V(\vec{k},\vec{k}\,';\vec{q}\,) + \int d^3k'' \frac{V(\vec{k},\vec{k}\,'';\vec{q}\,)t(\vec{k}\,'',\vec{k}\,';\vec{q}\,)}{\sqrt{(2\omega(\vec{k}\,'))^2 + \vec{q}^{\,2}} - \sqrt{(2\omega(\vec{k}\,''))^2 + \vec{q}^{\,2}} + i\epsilon}.$$

Two-body t-matrix

Nonrelativistic LS eq.

$$t^{nr}(\vec{k},\vec{k}\,';E) = v^{nr}(\vec{k},\vec{k}\,') + \int d^3k'' \frac{v^{nr}(\vec{k},\vec{k}\,'')\, t^{nr}(\vec{k}\,'',\vec{k}\,';E)}{E - k''^2/m + i\epsilon}.$$

Relativistic LS eq.

$$\hat{t}(\vec{k},\vec{k}\,';\vec{q}\,) = v(\vec{k},\vec{k}\,') + \int d^3k'' \frac{v(\vec{k},\vec{k}\,'')\, \hat{t}(\vec{k}\,'',\vec{k}\,';\vec{q}\,)}{2\omega(\vec{k}\,') - 2\omega(\vec{k}\,'') + i\epsilon}.$$

Boosted relativisitic LS eq.

$$t(\vec{k},\vec{k}\,';\vec{q}\,) = V(\vec{k},\vec{k}\,';\vec{q}\,) + \int d^3k'' \frac{V(\vec{k},\vec{k}\,'';\vec{q}\,)\, t(\vec{k}\,'',\vec{k}\,';\vec{q}\,)}{\sqrt{(2\omega(\vec{k}\,'))^2 + \vec{q}^{\,2}} - \sqrt{(2\omega(\vec{k}\,''))^2 + \vec{q}^{\,2}} + i\epsilon}.$$

Two-body t-matrix

Nonrelativistic LS eq.

$$t^{nr}(\vec{k},\vec{k}\,';E) = v^{nr}(\vec{k},\vec{k}\,') + \int d^3k'' \frac{v^{nr}(\vec{k},\vec{k}\,'')\,t^{nr}(\vec{k}\,'',\vec{k}\,';E)}{E - k''^2/m + i\epsilon}.$$

Relativistic LS eq.

$$\hat{t}(\vec{k},\vec{k}\,';\vec{q}\,) = v(\vec{k},\vec{k}\,') + \int d^3k'' \frac{v(\vec{k},\vec{k}\,'')\,\hat{t}(\vec{k}\,'',\vec{k}\,';\vec{q}\,)}{2\omega(\vec{k}\,') - 2\omega(\vec{k}\,'') + i\epsilon}.$$

Boosted relativisitic LS eq.

$$t(\vec{k},\vec{k}\,';\vec{q}\,) = V(\vec{k},\vec{k}\,';\vec{q}\,) + \int d^3k'' \frac{V(\vec{k},\vec{k}\,'';\vec{q}\,)\,t(\vec{k}\,'',\vec{k}\,';\vec{q}\,)}{\sqrt{(2\omega(\vec{k}\,'))^2+\vec{q}^{\,2}} - \sqrt{(2\omega(\vec{k}\,''))^2+\vec{q}^{\,2}} + i\epsilon}.$$

Mass Operator

$$H_0 = \sqrt{(2\omega(\vec{k}))^2 + \vec{q}^{\,2}}$$

Two-body Free Hamiltonian
(Two-body Free Mass
operator)

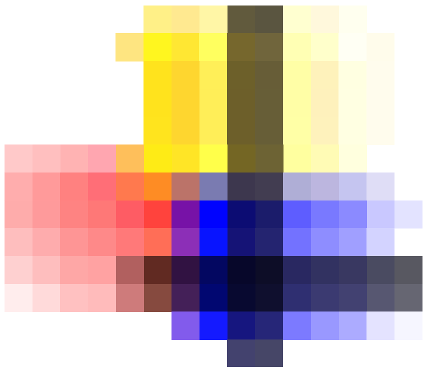

$$2\omega(\vec{k}) \equiv 2\sqrt{m^2 + \vec{k}^{\,2}}$$

Boosted Potential

$$V(\vec{q}) \equiv \sqrt{(\boxed{2\omega(\vec{k}) + v})^2 + \vec{q}^{\,2}} - \sqrt{(2\omega(\vec{k}))^2 + \vec{q}^{\,2}},$$

Two-body Mass operator

Two-body Free Mass operato

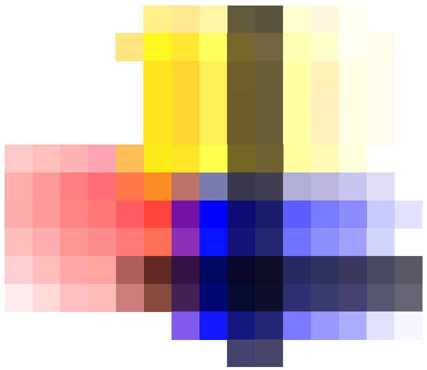

v : Relativistic potential

Boosted Potential

$$V(\vec{q}) \equiv \sqrt{(2\omega(\vec{k}) + v)^2 + \vec{q}^{\,2}} - \sqrt{(2\omega(\vec{k}))^2 + \vec{q}^{\,2}},$$

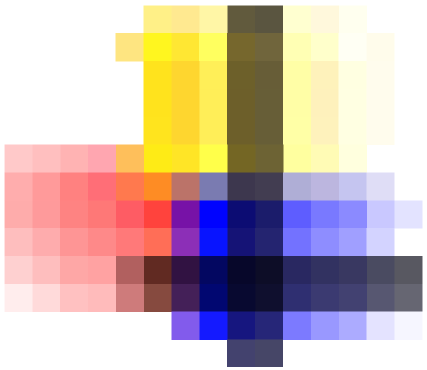

$$\begin{aligned}
&\langle \vec{k} | V(\vec{p}) | \vec{k}' \rangle \\
&= \psi_b(\vec{k}) \sqrt{M_b^2 + p^2}\, \psi_b(\vec{k}') \\
&\quad + \frac{t^*(\vec{k}', \vec{k}; \omega)}{\omega - \omega' - i\epsilon} \sqrt{\omega^2 + p^2} + \frac{t(\vec{k}, \vec{k}'; \omega')}{\omega' - \omega + i\epsilon} \sqrt{\omega'^2 + p^2} \\
&\quad + \int d^3k'' \frac{t(\vec{k}, \vec{k}''; \omega'')}{\omega'' - \omega + i\epsilon} \sqrt{\omega''^2 + p^2}\, \frac{t^*(\vec{k}', \vec{k}''; \omega'')}{\omega'' - \omega' - i\epsilon}
\end{aligned}$$

Phys. Rev. C **66**, 044010 (2002)

"Scale-transform it from nonrelativity to relativity "

v (pseudo) Relativistic potential

$$v(\vec{k},\vec{k}\,') = \frac{1}{h(k_{nr})} v^{(nr)}(\vec{k}_{nr},\vec{k}\,'_{nr}) \frac{1}{h(k'_{nr})}$$

Scale transformation

$$k_{nr} \equiv |\,\vec{k}_{nr}\,| = \sqrt{2m}\sqrt{\sqrt{\vec{k}^{\,2}+m^2}-m}$$

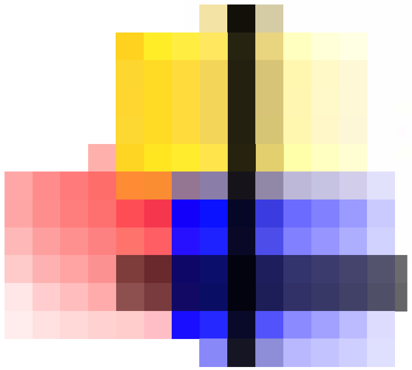

$$h(k_{nr}) = \sqrt{(1+\frac{k_{nr}^2}{2m^2})\sqrt{1+\frac{k_{nr}^2}{4m^2}}}.$$

Phys. Rev. Lett. **80,** 2457(1998)

$$\left(\frac{\hat{k}^2}{m} + V_{nr}\right)\Psi = \frac{k_0^2}{m}\Psi$$

$$E + 2m = 2\sqrt{m^2 + k_0^2}$$

This can be related to an underlying relativistic NN Schrödinger equation:

$$\left(2\sqrt{m^2 + \hat{k}^2} + \upsilon\right)\Psi = 2\sqrt{m^2 + \hat{k}_0^2}\,\Psi$$

by a simple algebra step. Make eq. (2) square then, we get

$$\left(4(\cancel{m}^2 + \hat{k}^2) + 2\sqrt{m^2 + \hat{k}^2}\,\upsilon + 2\upsilon\sqrt{m^2 + \hat{k}^2} + \upsilon^2\right)\Psi$$

$$= 4(\cancel{m}^2 + k_0^2)\Psi$$

which can be identically rewritten into (1) if one defines

Coester-Pieper-Serduke (CPS)

$$V_{nr} \equiv \frac{1}{4m}\left(2\sqrt{m^2 + \hat{k}^2}\,\upsilon + 2\upsilon\sqrt{m^2 + \hat{k}^2} + \upsilon^2\right)$$

(PRC11, 1 (1975))

$$V_{\mathrm{nr}} = \frac{1}{4m}\left(2\omega(\hat{k})v + 2v\omega(\hat{k}) + v^2\right) \tag{4}$$

Sandwiching it between <k | and |k'>, we get

$$V_{nr}(k,k') = \frac{1}{4m}\left(2\omega(k)v(k,k') + 2v(k,k')\omega(k') + \int v(k,k'')v(k'',k')d^3k''\right)$$

$$= \frac{1}{2m}\big(\omega(k) + \omega(k')\big)v(k,k') + \frac{1}{4m}\int v(k,k'')v(k'',k')d^3k''$$

namely,

$$v(k,k') = \frac{1}{\omega(k) + \omega(k')}\left(2mV_{nr}(k,k') - \frac{1}{2}\int v(k,k'')v(k'',k')d^3k''\right).$$

$$v(k,k') = \frac{1}{\omega(k)+\omega(k')}\left(2mV_{nr}(k,k') - \frac{1}{2}\int v(k,k'')v(k'',k')d^3k''\right).$$

Iteration Method

$$v(k,k')^{(0)} = \frac{1}{\omega(k)+\omega(k')}2mV_{nr}(k,k'),$$

$$v(k,k')^{(n+1)} = \frac{1}{\omega(k)+\omega(k')}\left(2mV_{nr}(k,k') - \frac{1}{2}\int v(k,k'')^{(n)}v(k'',k')^{(n)}d^3k''\right)$$

Physics Letters **B655**, 119-125 (2007), (nucl-th/0703010)

Convergence to the iteration

TABLE I: Convergence of $v^{(n)}$ to the iteration in Eq. (15). We choose the coupled partial waves ($^3S_1$-$^3D_1$) of the Argonne V18 potential[1]. The momenta k and k' are 1.0 fm^{-1} and the potential unit is [fm^2].

n	$v^{(n)}(^3S_1\text{-}^3S_1)$	$v^{(n)}(^3S_1\text{-}^3D_1)$	$v^{(n)}(^3D_1\text{-}^3D_1)$
0	0.084232	0.044709	0.016853
1	0.067716	0.044628	0.016785
2	0.059933	0.044597	0.016744
3	0.056135	0.044587	0.016719
4	0.054234	0.044585	0.016705
5	0.053259	0.044587	0.016696
6	0.052749	0.044589	0.016691
10	0.052194	0.044595	0.016684
20	0.052126	0.044597	0.016684
30	0.052126	0.044597	0.016684

TABLE II: Comparison of the phase shift and the mixing parameters
for the coupled partial waves ($^3S_1$-$^3D_1$) of the Argonne V18 potential[1]. The second column points to the relativistic (Rel.) or nonrelativistic (Nonrel.) calculations. The unit of the phases are in degrees.

$T_{lab.}$ [MeV]	Nonrel./Rel.	$\delta(^3S_1)$	$\delta(^3D_1)$	ϵ
1.0	Nonrel.	147.62	-0.0050743	0.10303
1.0	Rel.	147.62	-0.0050744	0.10304
10.0	Nonrel.	102.71	-0.66593	1.1267
10.0	Rel.	102.71	-0.66593	1.1267
50.0	Nonrel.	62.929	-6.3189	2.0853
50.0	Rel.	62.929	-6.3189	2.0854
100.0	Nonrel.	43.531	-12.093	2.4899
100.0	Rel.	43.531	-12.093	2.4899
350.0	Nonrel.	2.6451	-26.719	4.9223
350.0	Rel.	2.6452	-26.719	4.9222

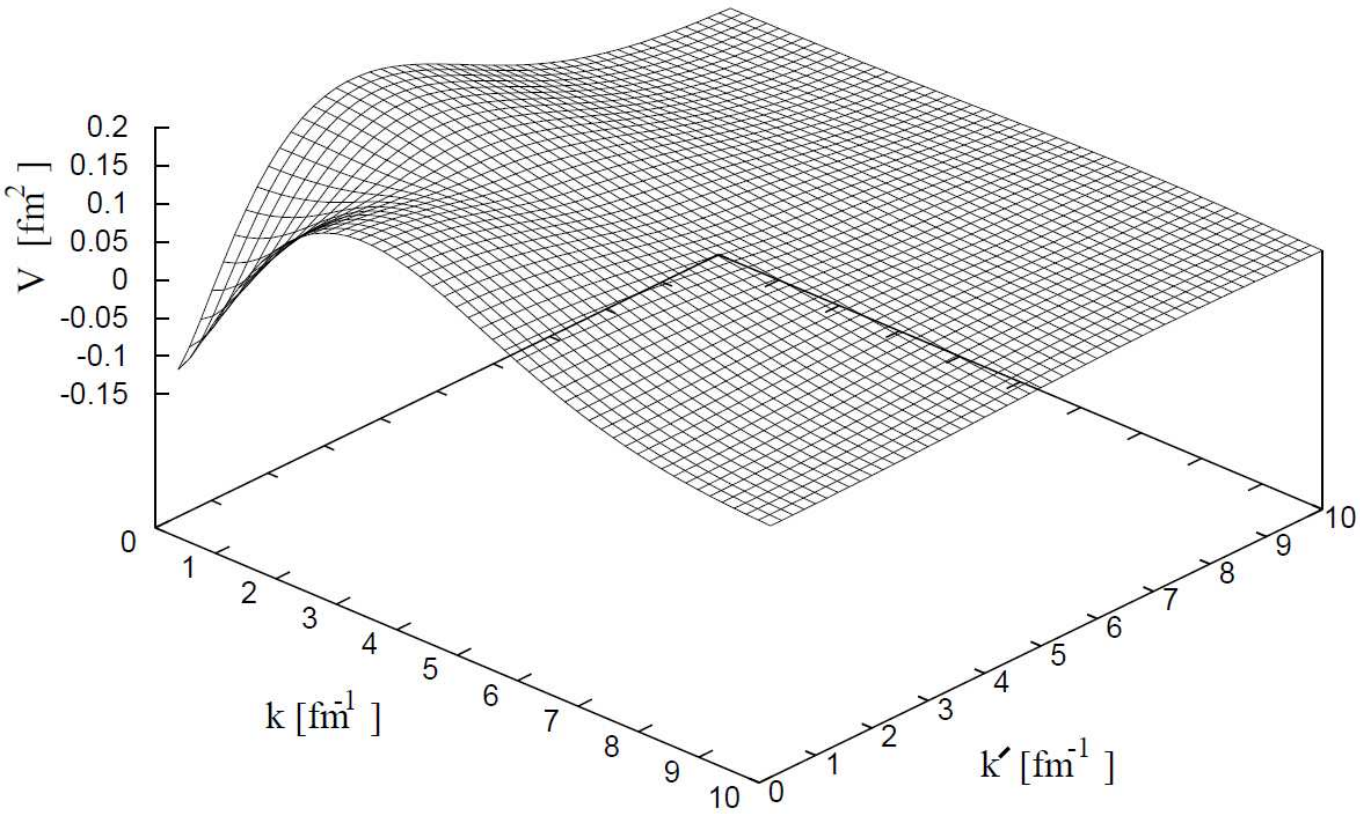

FIG. 1: Nonrelativistic potential $V(k,k')$ of AV18. The partial wave is chosen as $^1S_0$.

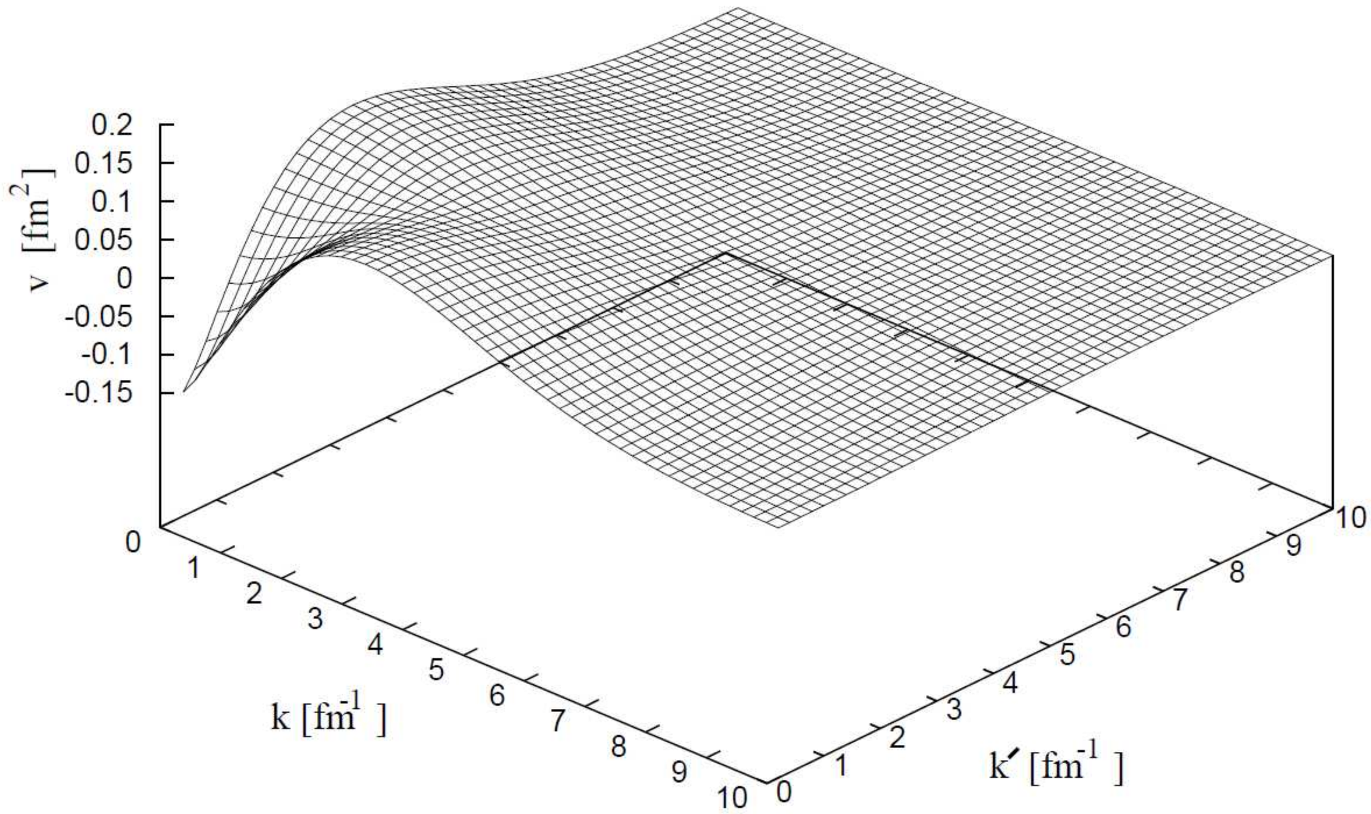

FIG. 2: Relativistic potential $v(k, k')$ of AV18. The partial wave is chosen as ${}^1S_0$.

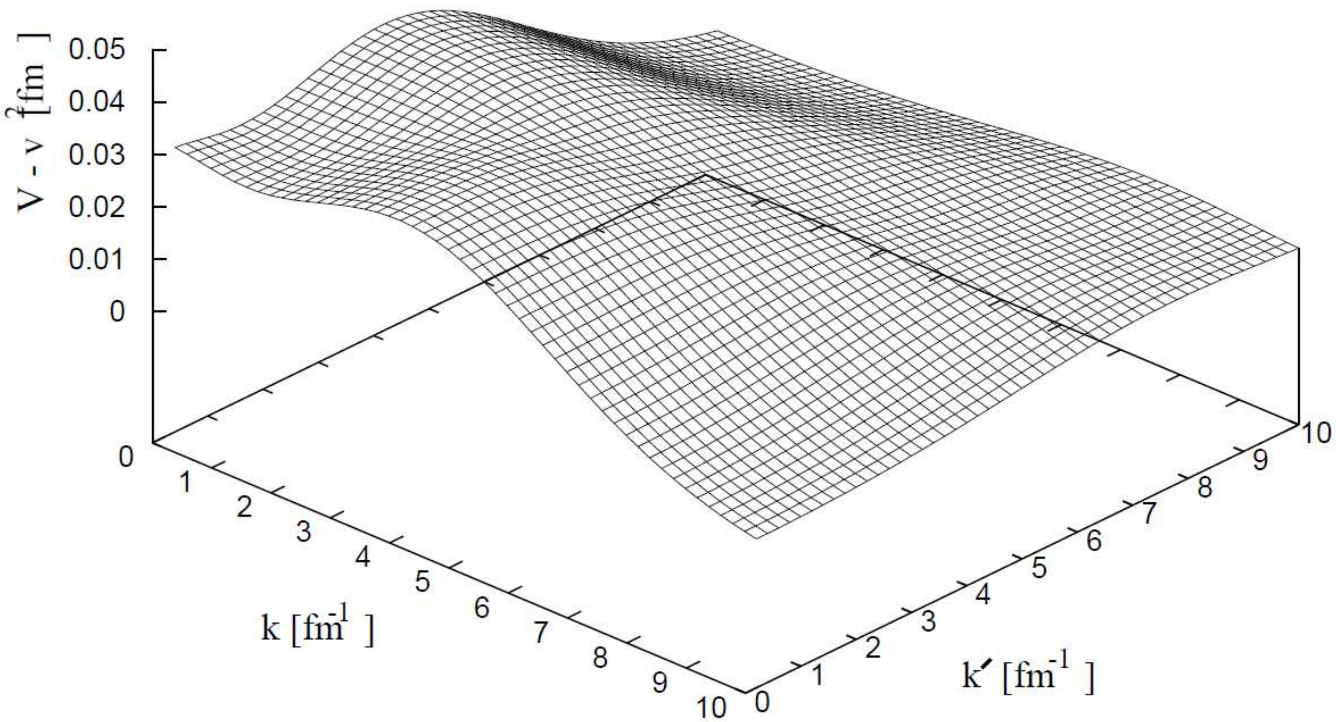

FIG. 3: Difference between relativistic and nonrelativistic potential $V(k,k') - v(k,k')$. The partial wave is chosen as ${}^1S_0$.

$$2\omega_q(k) \equiv \sqrt{\{2\omega(k)\}^2 + q^2}$$

Boosted

$$v_q(k,k') = \frac{1}{\omega_q(k)+\omega_q(k')}\left(2mV_{nr}(k,k') - \frac{1}{2}\int v_q(k,k'')v_q(k'',k')d^3k''\right).$$

$$v(k,k') = \frac{1}{\omega(k)+\omega(k')}\left(2mV_{nr}(k,k') - \frac{1}{2}\int v(k,k'')v(k'',k')d^3k''\right).$$

Non-boosted

→ **Iteration method**

Calculation of triton binding energy

- No Wigner Rotation
- Wigner Rotation (Lorentz transform on Spin)

Triton binding energies (No Wigner Rotation)

Interaction	Rel.	Nonrel.	Δ
RSC	−6. 97	−7. 02	0. 05
CD-Bonn	−8. 22	−8. 33	0. 11
Nijmegen II	−7. 58	−7. 65	0. 07
Nijmegen I	−7. 90	−8. 00	0. 10
Nijmegen 93	−7. 68	−7. 76	0. 08
AV18	−7. 59	−7. 66	0. 07
expt.	−8.48		

5ch calculation

The relativistic results are;

Using only np force (in MeV) ...

potential	5ch	18ch	26ch	34ch
RSC	-6.971	-7.153	-	-
CDBonn	-8.219	-8.123	-8.143	-8.147
Nijm I	-7.899	-7.868	-7.900	-7.905
Nijm II	-7.583	-7.690	-7.756	-7.769
Nijm 93	-7.684	-7.688	-7.750	-7.759
AV18	-7.589	-7.649	-7.717	-7.725

Using np force + nn force [1/3-2/3 rule] (in MeV)

potential	5ch	18ch	26ch	34ch
CDBonn	-7.9842	-7.8914	-7.9119	-7.9157
Nijm I	-7.6214	-7.5956	-7.6282	-7.6331
Nijm II	-7.3421	-7.4419	-7.5060	-7.5181
Nijm 93	-7.4753	-7.4834	-7.5447	-7.5536
AV18	-7.3431	-7.4029	-7.4703	-7.4790

Wigner Rotation
(Lorentz transformation on Spin)

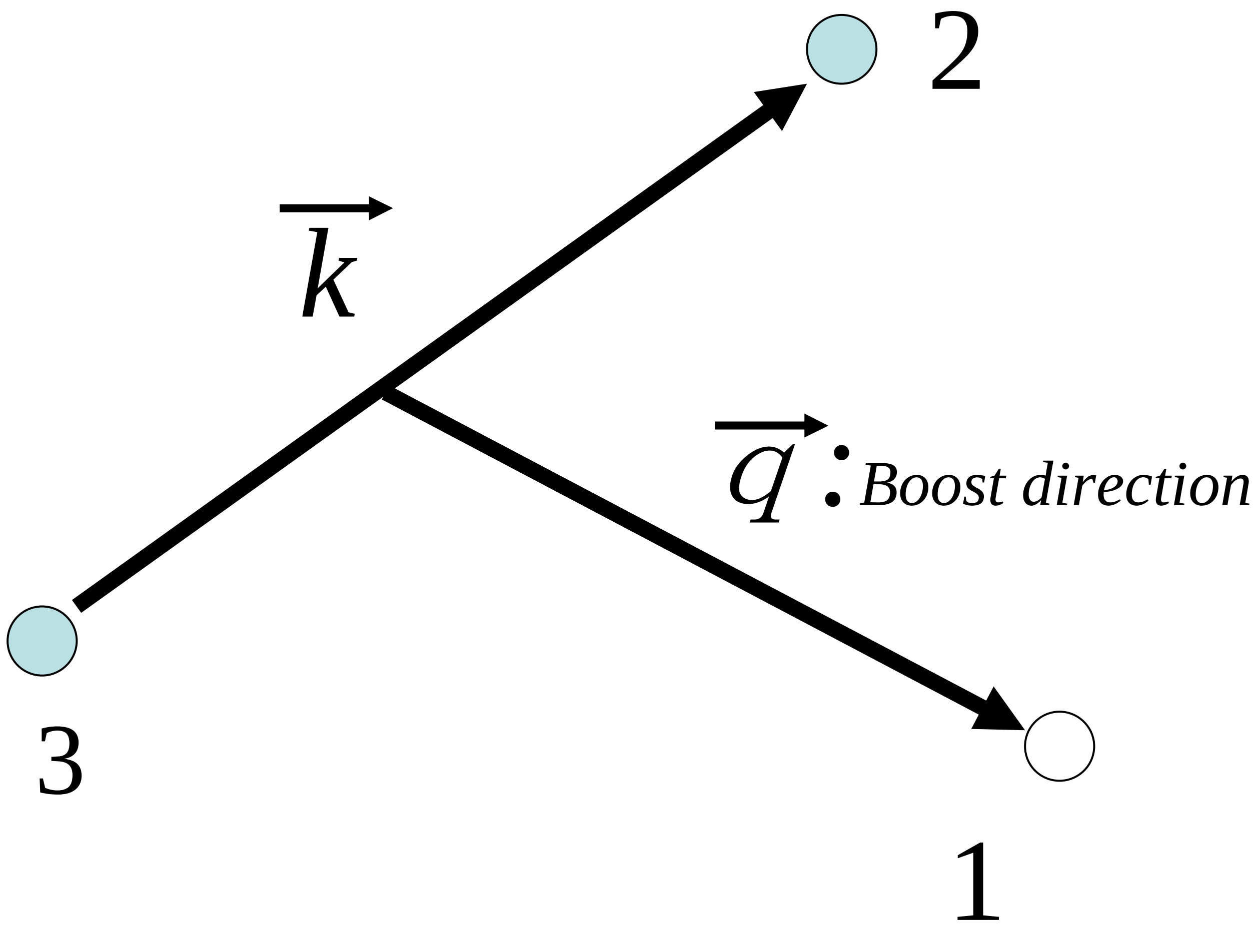

2
$\vec{k}$
$\vec{q}$: Boost direction
3
1

Partial wave decomposition

$$|kq = p_1\alpha > \;\equiv\; |kp_1(ls)j(\lambda\frac{1}{2})I(jI)JM > |(t\frac{1}{2})TM_T >$$

$$= N(\vec{p}_2,\vec{p}_3) \sum_{\mu_2\mu_3\mu_s} \sum_{\mu_l{\mu'}_2{\mu'}_3} \sum_{\mu_1\mu_\lambda\mu_I\mu} (\frac{1}{2}\mu_2\frac{1}{2}\mu_3|s\mu_s)(l\mu_l s\mu_s|j\mu)(\lambda\mu_\lambda\frac{1}{2}\mu_1|I\mu_I)(j\mu I\mu_I|JM)$$
$$\int d\hat{p}_1 Y^{\lambda}_{\mu_\lambda}(\hat{p}_1) \int d\hat{k} Y^{l}_{\mu_l}(\hat{k}) D^{\frac{1}{2}}_{{\mu'}_2\mu_2}(R(\beta(P),\vec{k}))\; D^{\frac{1}{2}}_{{\mu'}_3\mu_3}(R(\beta(P),-\vec{k}))|(t\frac{1}{2})TM_T >$$
$$|\vec{p}_2{\mu'}_2\vec{p}_3{\mu'}_3\vec{p}_1\mu_1 > .$$

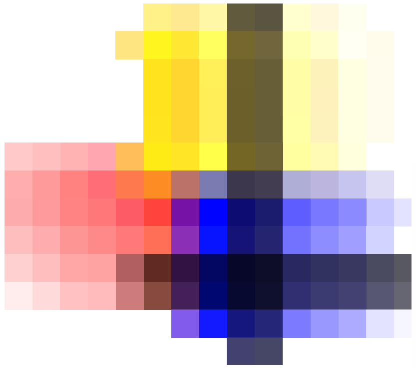

Here $D^{\frac{1}{2}}_{\mu'\mu}$ are the standard SU(2) Wigner D-matrices

$$|\frac{\partial(\vec{p}_2\;\vec{p}_3)}{\partial(\vec{P}\;\vec{k})}| = \frac{M_0}{\omega_{M_0}(\vec{P})}\frac{\omega_m(\vec{p}_2)}{\omega_m(\vec{k})}\frac{\omega_m(\vec{p}_3)}{\omega_m(\vec{k})} \equiv N^2(\vec{p}_2,\vec{p}_3)$$

Effect of Wigner Rotation

34ch Calculation with CD－Bonn (np)

Nonrel.	Relativistic (non-Wigner Rotation)	Relativistic (Wigner Rotation)
－8．247	－8．1459MeV	－8．1443MeV

Difference ～2keV

Calculation of triton binding energy

- The iteration method makes the relativistic potential to boost directly. The calculation of triton binding energies shows differences between the nonrelativistic and relativistic about 100keV. ($|E_{nr}|>|E_{rel}|$)

- The Wigner rotation makes effects about only 2.～4. keV.

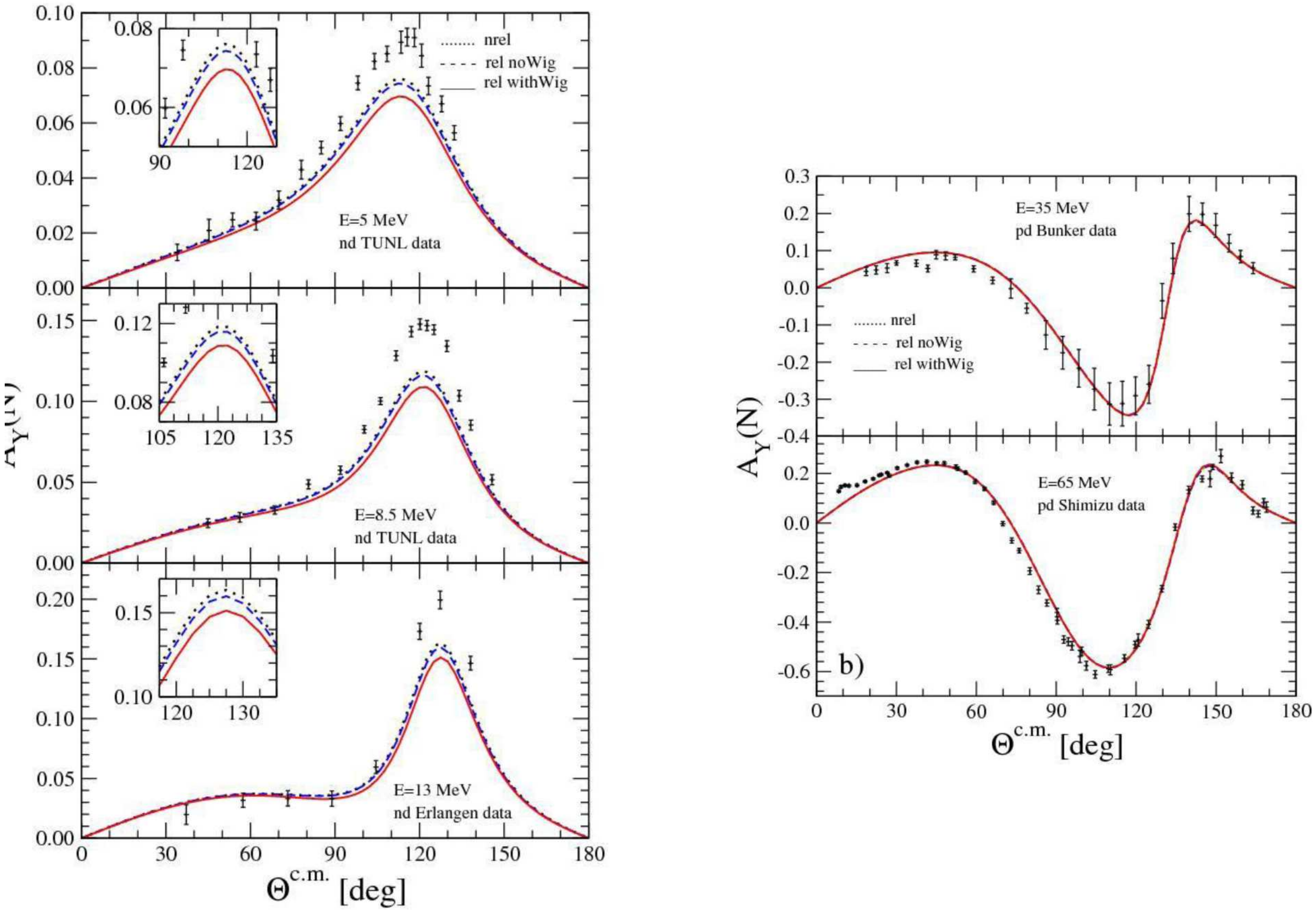

nrel
rel noWig
rel withWig
E=5 MeV
nd TUNL data
E=8.5 MeV
nd TUNL data
E=13 MeV
nd Erlangen data
E=35 MeV
pd Bunker data
E=65 MeV
pd Shimizu data
b)
$A_Y(N)$
$\Theta^{c.m.}$ [deg]

E(lab)=200MeV.

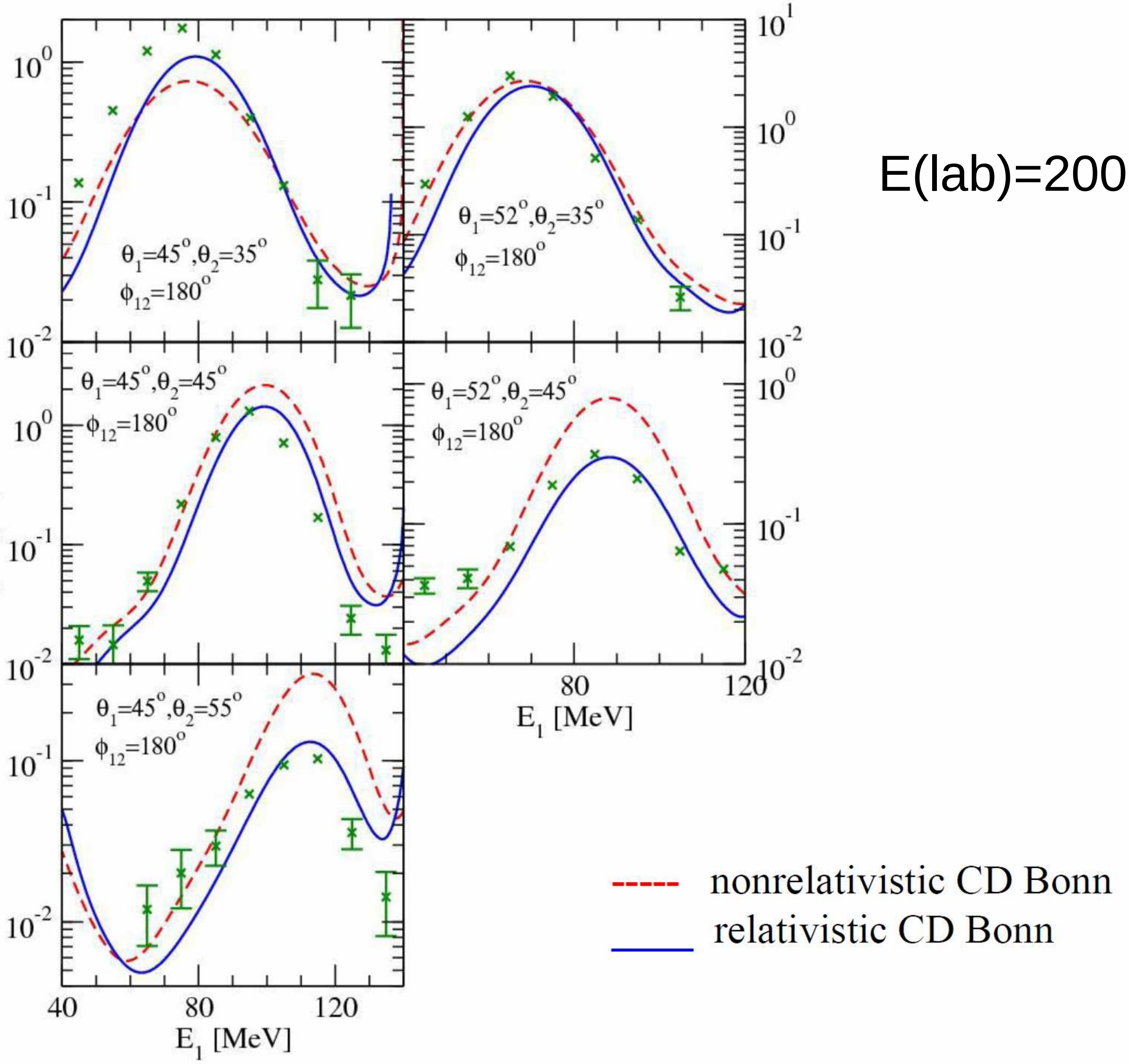

θ1=45°,θ2=35°
φ12=180°
θ1=52°,θ2=35°
φ12=180°
θ1=45°,θ2=45°
φ12=180°
θ1=52°,θ2=45°
φ12=180°
θ1=45°,θ2=55°
φ12=180°
E1 [MeV]
nonrelativistic CD Bonn
relativistic CD Bonn

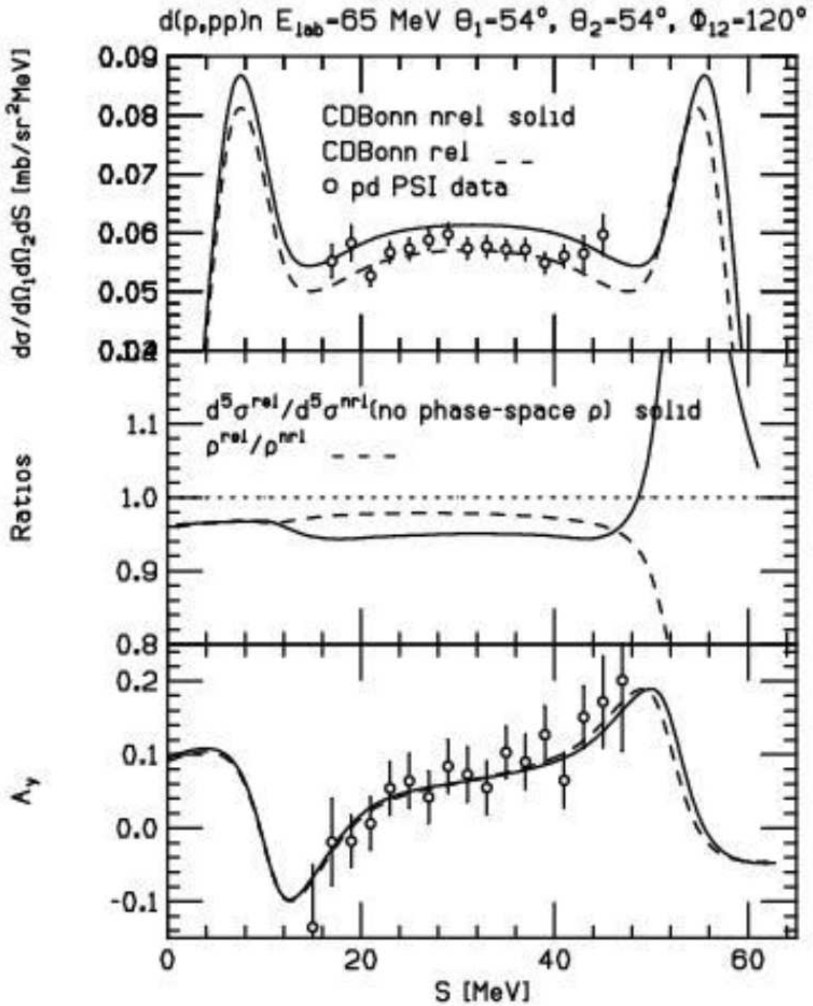

d(p,pp)n E_lab=65 MeV θ1=54°, θ2=54°, Φ12=120°
dσ/dΩ1dΩ2dS [mb/sr^2MeV]
CDBonn nrel solid
CDBonn rel
pd PSI data
d^5σ^rel/d^5σ^nrl(no phase-space ρ) solid
ρ^rel/ρ^nrl
Ratios
A_y
S [MeV]

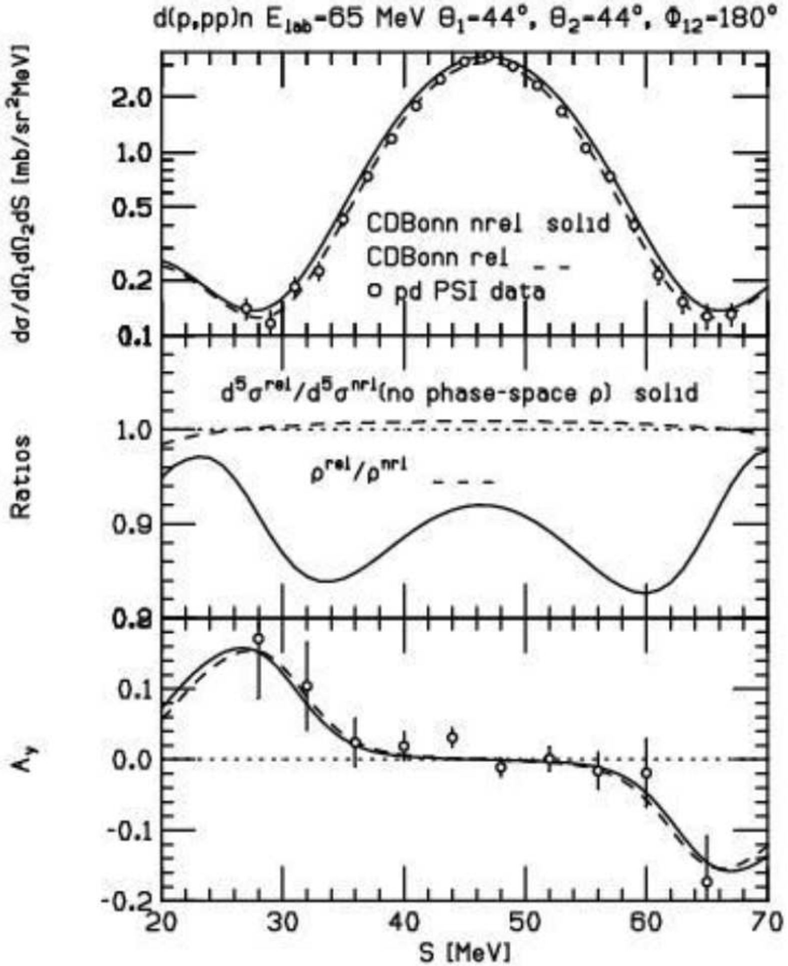

d(p,pp)n E_lab=65 MeV θ1=44°, θ2=44°, Φ12=180°
dσ/dΩ1dΩ2dS [mb/sr^2MeV]
CDBonn nrel solid
CDBonn rel
pd PSI data
d^5σ^rel/d^5σ^nrl(no phase-space ρ) solid
ρ^rel/ρ^nrl
Ratios
A_y
S [MeV]

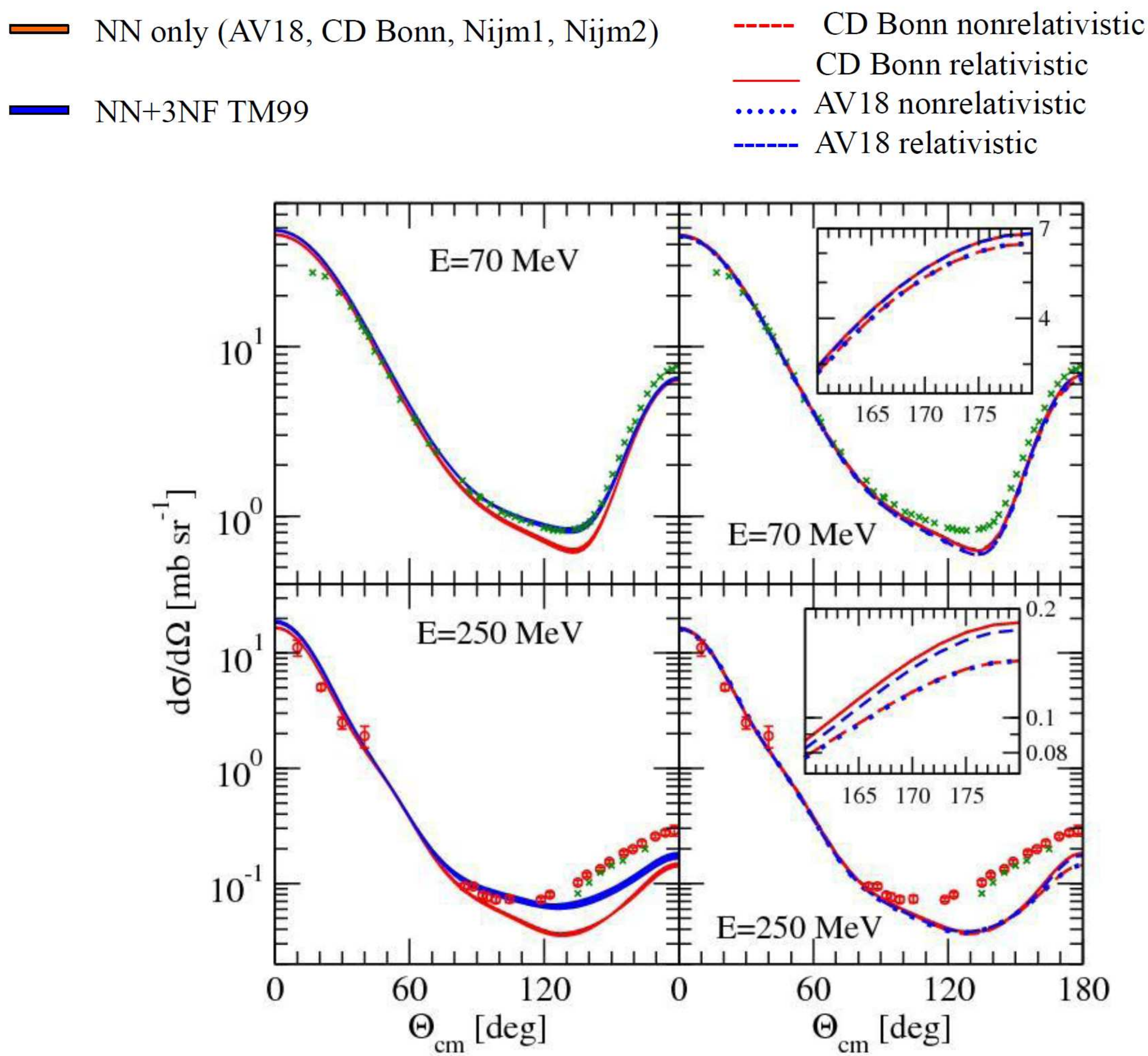

NN only (AV18, CD Bonn, Nijm1, Nijm2)
NN+3NF TM99
CD Bonn nonrelativistic
CD Bonn relativistic
AV18 nonrelativistic
AV18 relativistic
E=70 MeV
E=70 MeV
E=250 MeV
E=250 MeV
dσ/dΩ [mb sr^-1]
Θ_cm [deg]
Θ_cm [deg]

Calculation of Nd scattering

- 低エネルギー（50MeVまで）のオブザーバブルは変わらない。Observables in low energy (~50MeV) are well described as nonrelativistic calculation except for Ay.
- 例外：Ay
- 250MeVの微分断面積の後方散乱角で実験に近づく兆しがある。（3体力なし）The calculated differential cross section is approaching data a bit at the backwards scattering angles.
- しかし、3体力の効果を単に加算しても十分に実験を再現しない見通し(!?)。It seems to be difficult to describe data even including 3NF.

News 2

- ３体力を含めた相対論的計算が可能になる。The recent progress is that we have the relativistic calculation of Faddeev equation including 3NF.: Phy. Rev. C **83**, 044001 (2011) ; arXiv:1101.4053 [nucl-th].
- ３体力を加えると、後方の微分断面積を相乗的に増加させる効果があることが分かった。The relativity and 3NF makes the differential cross section enlarge synergistically.

PHYSICAL REVIEW C **83**, 044001 (2011)

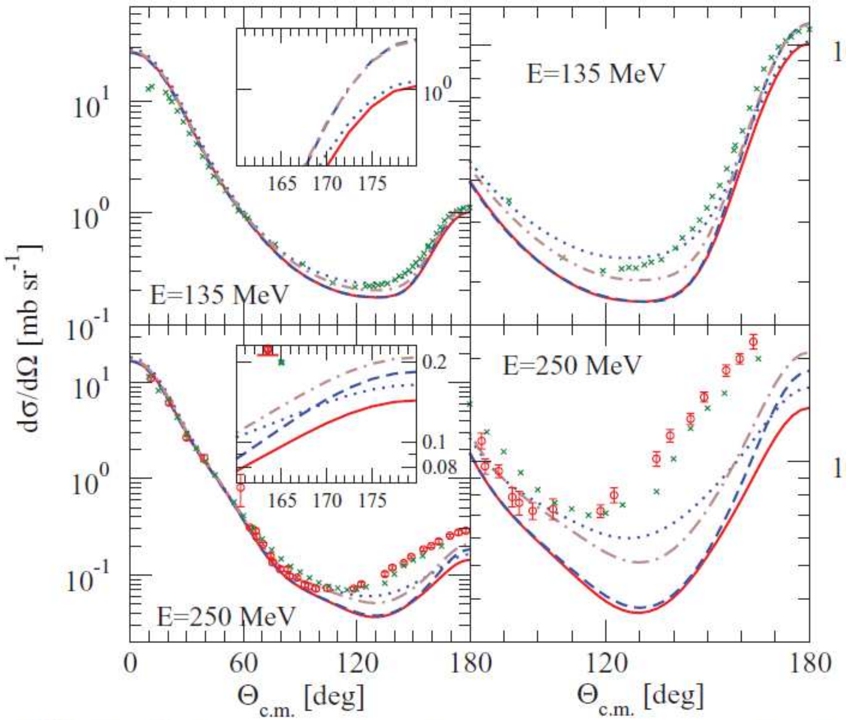

FIG. 4. (Color online) The elastic nd scattering angular distributions at the incoming neutron laboratory energy $E = 135$ and 250 MeV. The solid (red) and dotted (blue) lines are results of the nonrelativistic Faddeev calculations with the CD Bonn potential alone and combined with TM99 three-nucleon force, respectively. The relativistic predictions based on CD Bonn potential without Wigner spin rotations are shown by the dashed (blue) lines. The dashed-dotted (brown) lines show results of relativistic calculations with the TM99 three-nucleon force included. The pd data (×) at 135 MeV are from Ref. [7] and at 250 MeV from Ref. [37]. At 250 MeV also nd data of Ref. [36] are shown by circles. The inserts and figures in the right-hand column display details of the cross sections in specific angular ranges.

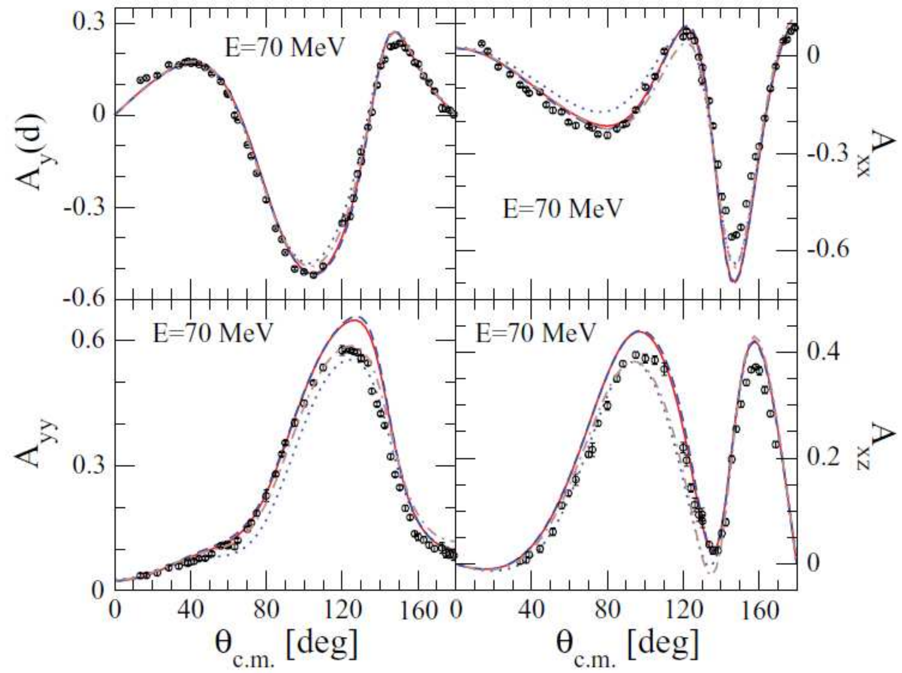

FIG. 5. (Color online) The vector (deuteron) $A_y(d)$ and tensor analyzing powers A_{xx}, A_{yy}, and A_{xz} in elastic nd scattering at the incoming neutron laboratory energy $E = 70$ MeV. For description of lines, see Fig. 4. The pd data (open circles) are from Ref. [7].

2NF ONLY-NONREL.

2NF ONLY-REL.

2NF+3NF NONREL.

2NF+3NF REL.

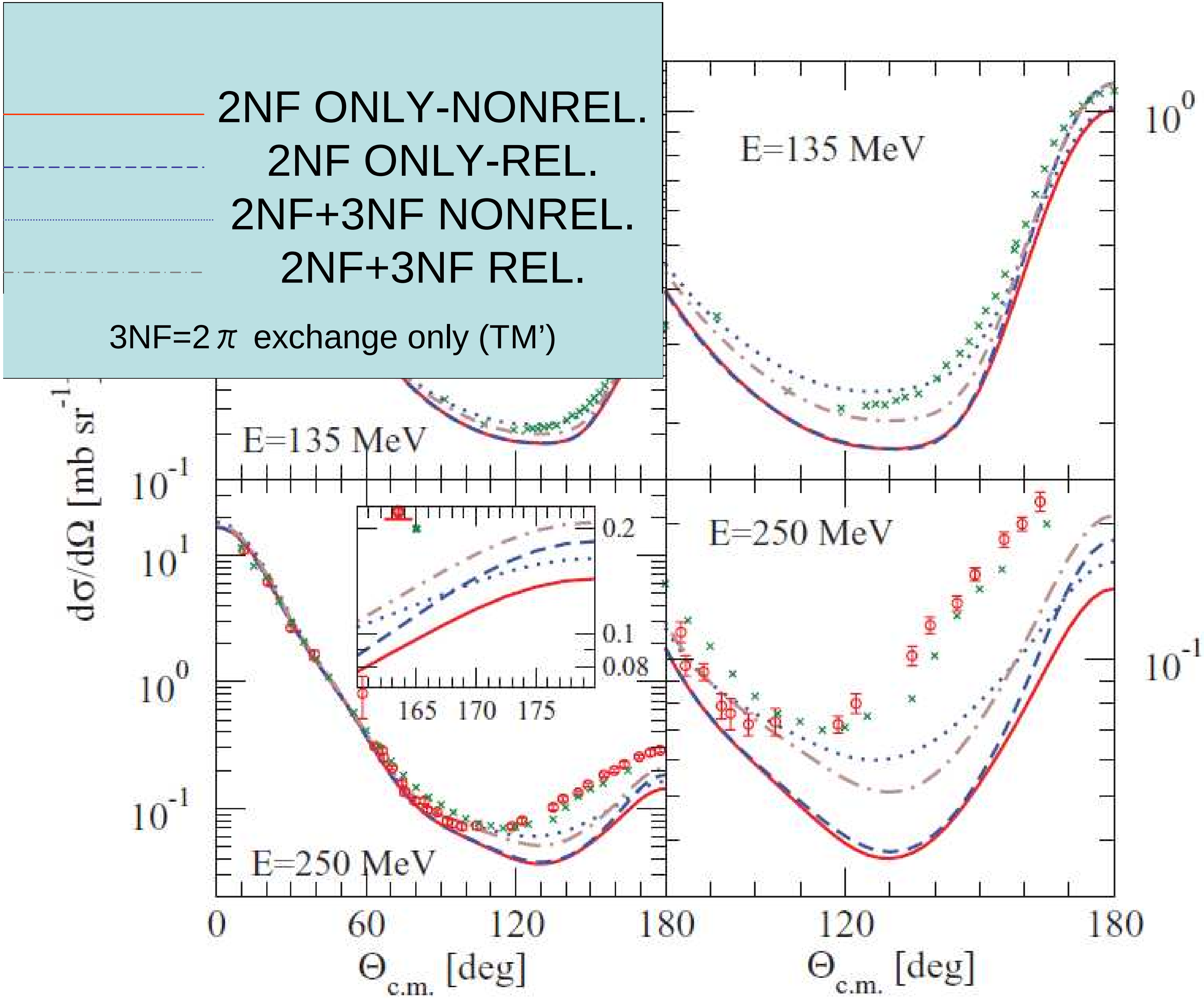
2NF ONLY-NONREL.
2NF ONLY-REL.
2NF+3NF NONREL.
2NF+3NF REL.
3NF=2π exchange only (TM')
E=135 MeV
E=135 MeV
E=250 MeV
E=250 MeV
dσ/dΩ [mb sr⁻¹]
Θc.m. [deg]
Θc.m. [deg]
0
60
120
180
120
180
10⁻¹
10¹
10⁰
10⁻¹
10⁰
10⁻¹
0.2
0.1
0.08
165
170
175

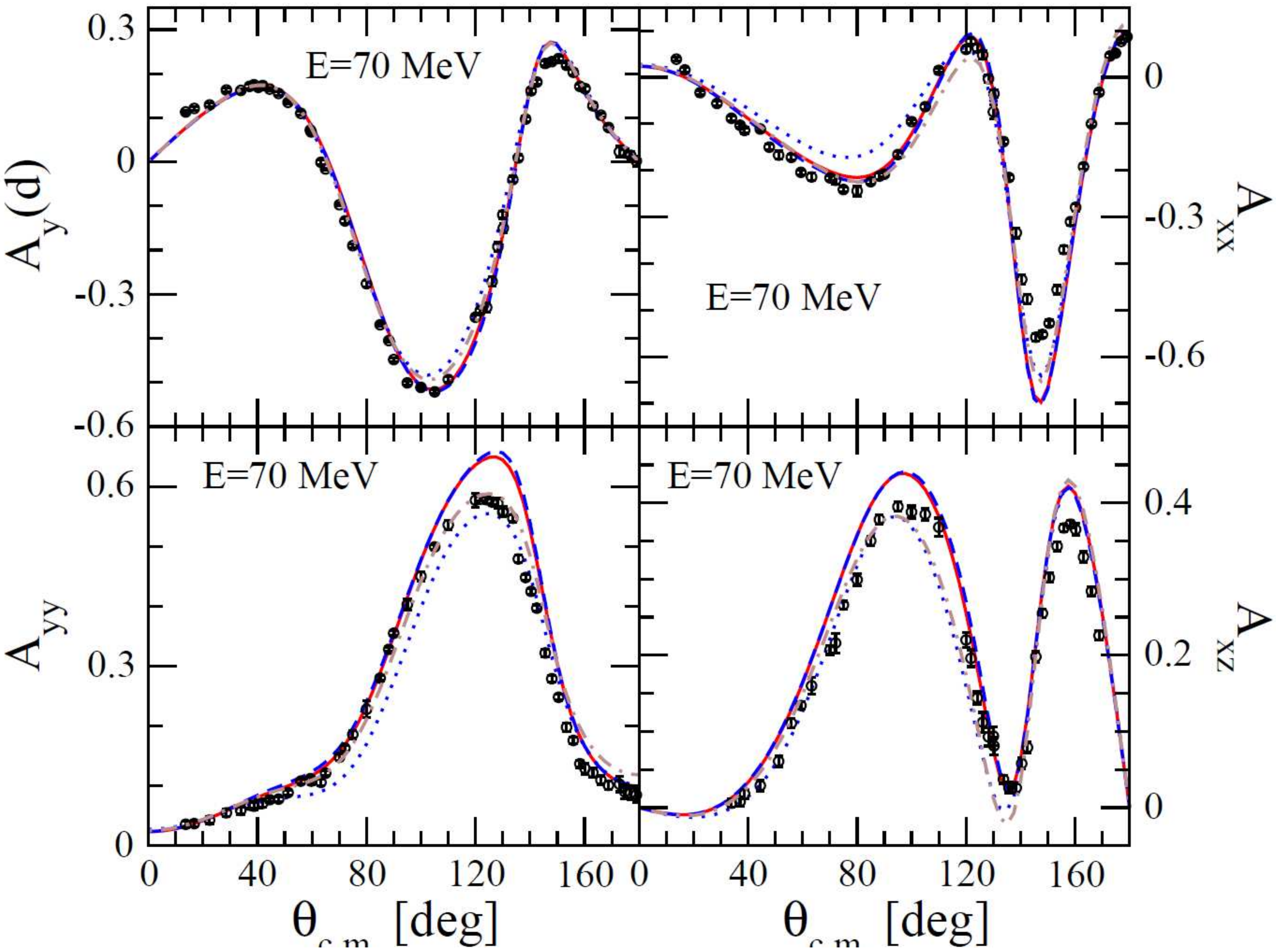

E=70 MeV
E=70 MeV
E=70 MeV
E=70 MeV
$A_y(d)$
A_{xx}
A_{yy}
A_{xz}
0.3
0
-0.3
-0.6
0
-0.3
-0.6
0.6
0.3
0
0.4
0.2
0
0
40
80
120
160
0
40
80
120
160
$\theta_{c.m.}$ [deg]
$\theta_{c.m.}$ [deg]

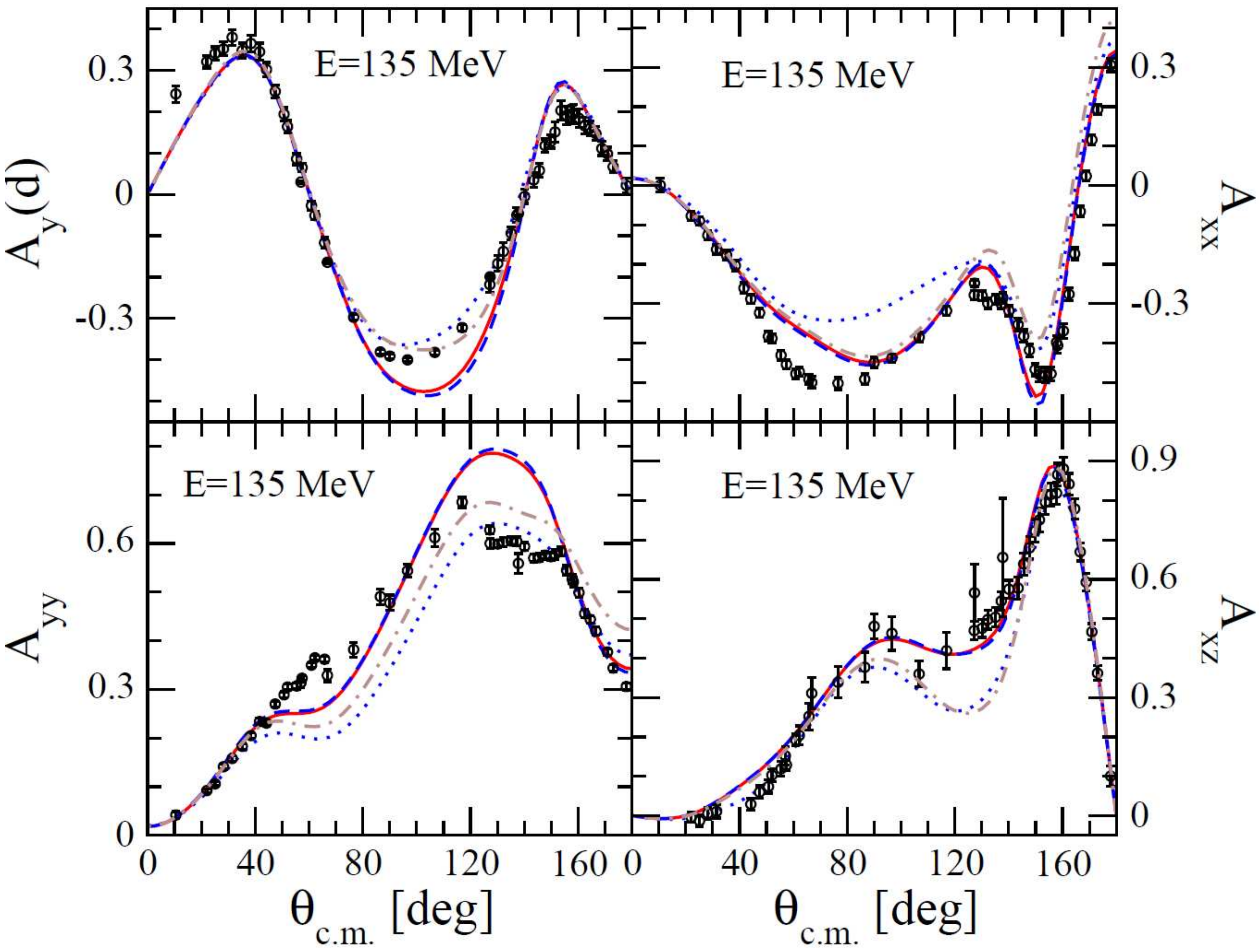

E=135 MeV
E=135 MeV
E=135 MeV
E=135 MeV
$A_y(d)$
A_{xx}
A_{yy}
A_{xz}
$\theta_{c.m.}$ [deg]
$\theta_{c.m.}$ [deg]

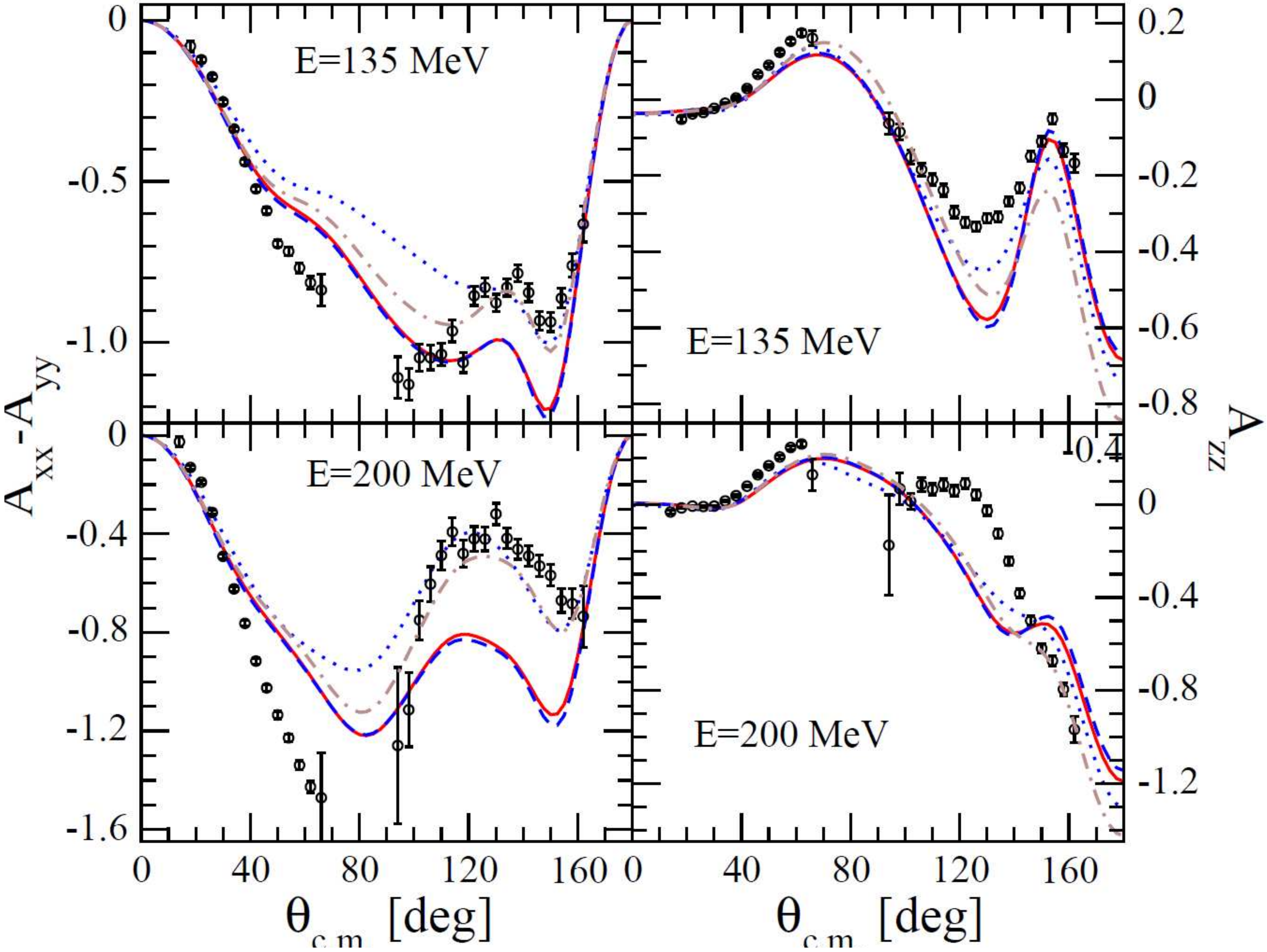

E=135 MeV
E=200 MeV
E=135 MeV
E=200 MeV
$A_{xx}-A_{yy}$
A_{zz}
$\theta_{c.m.}$ [deg]
$\theta_{c.m.}$ [deg]

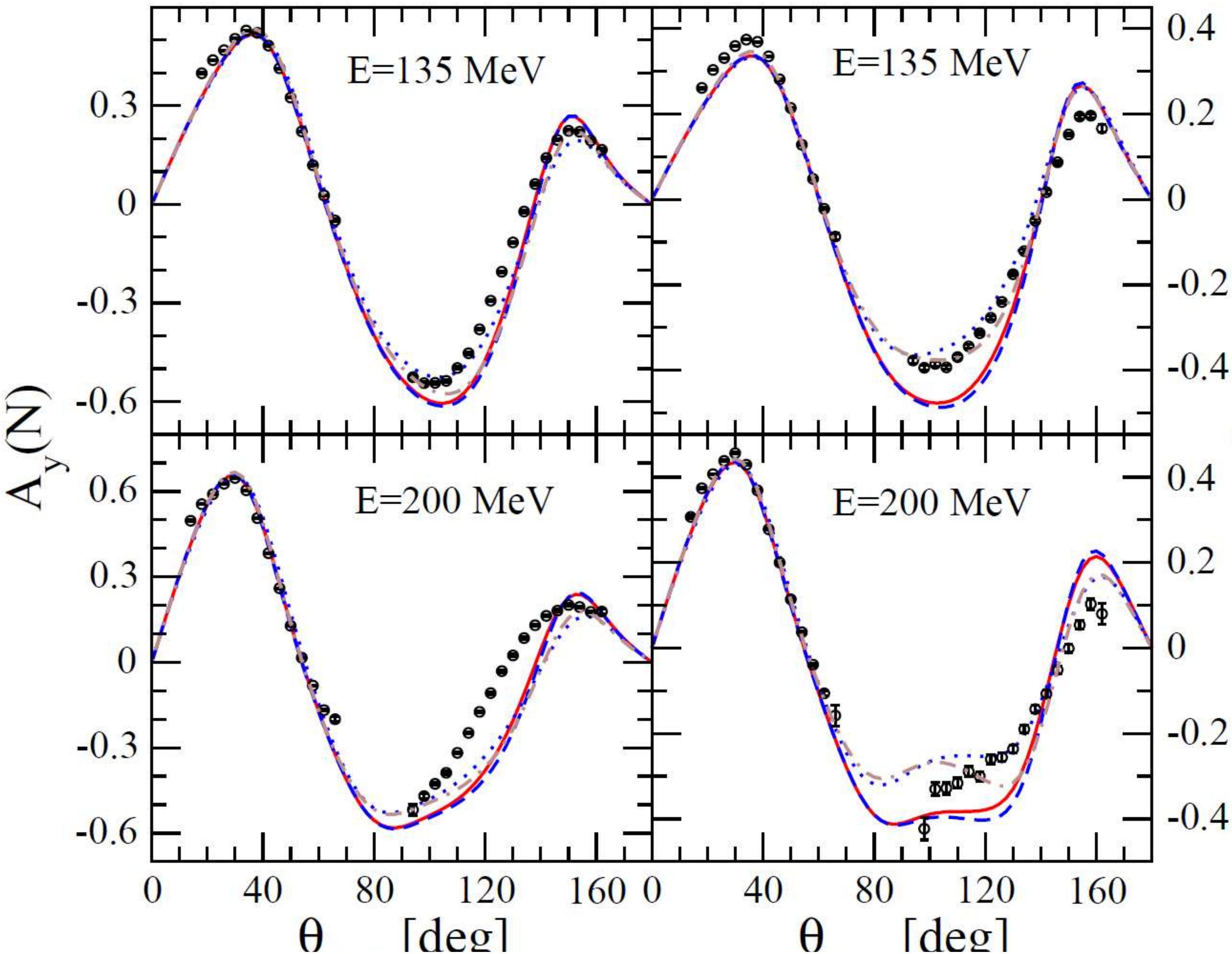

E=135 MeV
E=135 MeV
E=200 MeV
E=200 MeV
$A_y(N)$
$A_y(d)$
0.3
0
-0.3
-0.6
0.6
0.4
0.2
-0.2
-0.4
0
40
80
120
160
θ [deg]
θ [deg]

Outlook

- NNNLO calculations
- NNNLO+relativity calculations

→ Low energy:

(1) Ay puzzle

(2) Space star anomaly

(3) …

→ High energy:

(1) Differential cross section

(2) Spin Observables

Collaborators

W. Glöckle, E. Epelbaum, H. Krebs
(Ruhr-Universitaet Bochum, Germany)
H. Witala , J. Golak, R. Skibinski
(Jagiellonian University, Poland)
A. Nogga (Forschungszentrum Juelich, Germany)
W. Polyzou (The University of Aiowa, USA)

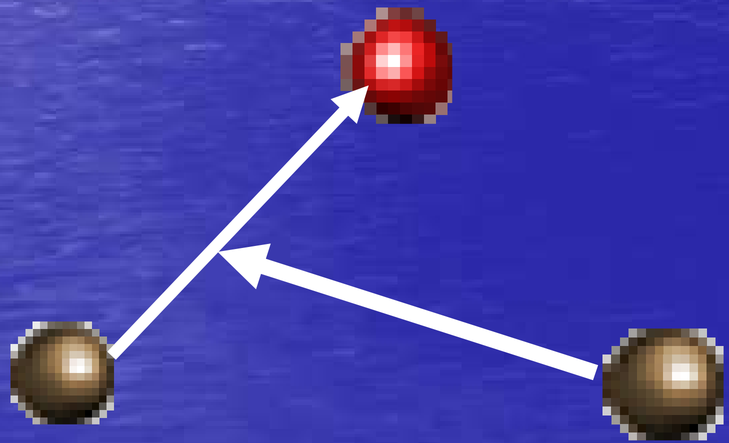

END